THE HIGHLY PREORGANIZED LIGANDS 1,10-PHENANTHROLINE-2,9-DIALDOXIME AND BIS-1,10-PHENANTHROLINE, AND THEIR COMPLEXING PROPERTIES WITH METAL IONS

Lindsay Leighton Boone

A Thesis Submitted to the
University of North Carolina Wilmington in Partial Fulfillment
Of the Requirements for the Degree of
Master of Science

Department of Chemistry

University of North Carolina Wilmington

2006

Approved by

Advisory Committee

_____ _____

_____
Chair

Accepted by

_____
Dean, Graduate School

TABLE OF CONTENTS

ABSTRACT

Preorganization is important in the recognition of metal ions by ligands. A ligand is more preorganized the more it is constrained as the free ligand to be in the conformation required to complex the target metal ion. Until the present time, high levels of preorganization have been achieved by cyclization of open-chain ligands to yield macrocycles and cryptands. A novel approach to designing highly preorganized ligands is followed where high levels of preorganization are achieved using the rigid 1,10-phenanthroline (1,10-phen) delocalized system as the backbone of the ligand. The highly preorganized ligands 1,10-phenanthroline-2,9-dialdoxime (PDOX) and bis-1,10-phenanthroline (DIPHEN) and their complexing properties with various metal ions have been studied.

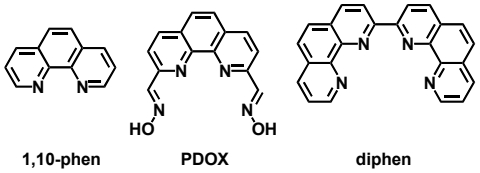

PDOX was synthesized by a literature method. Column chromatography of the product obtained by this method gave a product of improved purity, as shown by NMR and IR, and a considerably higher melting point. UV/VIS spectrometry was used in titrations to determine protonation constants of the free ligands and their stability constants with metal ions. Stability constants, $\log K_1$, for PDOX and DIPHEN with Ca(II), Cd(II), Cu(II), Gd(III), Pb(II), and Zn(II) have been determined. Fluorescence properties of PDOX and Ca(II), Cd(II), Pb(II), Hg(II), and Zn(II) were examined. The strong chelation enhanced fluorescence (CHEF) effect found with PDOX and metal ions such as Cd(II) and Pb(II) suggest that these ligands will have potential applications in biology, and in the development of sensors for these metal ions in the environment.

ACKNOWLEDGEMENTS

I would like to thank Dr. Robert Hancock for giving me the opportunity to work in his research group and for all the time and effort he has put into enriching my understanding of chemistry. I would also like to thank Dr. John Tyrell who always took the time to answer questions concerning my research as well as many other topics. Thank you, Dr. Sridhar Varadarajan for sharing your knowledge and advice with me it has been greatly appreciated. I would like to thank my lab groups who have become some of the best friends I have ever had.

I would like to acknowledge my mother and father, Kathy and Leon Boone, for supporting my decision to continue my education and being there for all the bumps in the road. Thank you a million times over to my grandparents, Tommye and Glen Pitman, for just loving me for who I am. Thank you to Travis Cook who has helped me to grow up in ways you will never know.

Finally, I would like to thank Texas Boone for being the best buddy a girl could have. You can always bring a smile to my face.

DEDICATION

I would like to dedicate this thesis to my grandmother, Leah Boone, who I love and miss very much. I hope she is proud of my accomplishments.

LIST OF TABLES

LIST OF FIGURES

INTRODUCTION

While the majority of target molecules for medicinal purposes are organic, inorganic molecules such as metal-ligand complexes also offer promise for the pharmaceutical industry. Metal-ligand complexes are being used in a wide variety of medicinal applications, such as MRI contrast agents, fluorescence detectors, and chelation therapies.[1,2,3] Therefore, ligand design and the stability of the metal-ligand complexes formed for these uses are of extreme importance. By examining these possible applications, insight can be obtained into what type of ligand would improve each process.

An MRI contrast agent shifts the MRI signal of the protons in water molecules. By shifting the signal of the protons in a water molecule, contrast is produced between high water content tissues such as plasma and low water content tissues such as fats. Currently, the most widely used contrasting agent is a diethylenetriamine pentaacetate (DTPA) complex with gadolinium (III) shown below.[4,5]

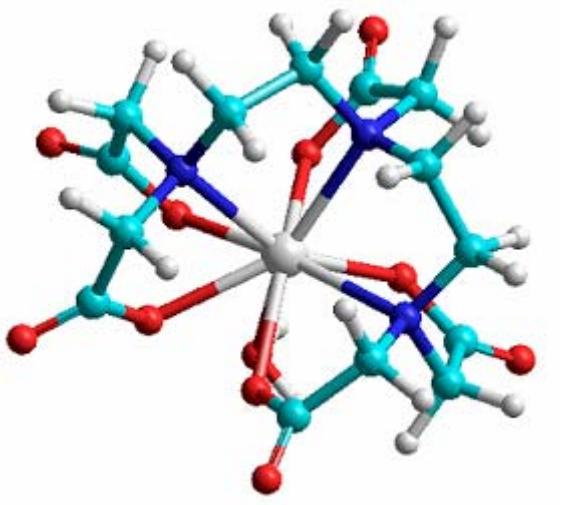

Gd^{3+}-DTPA Complex

Gadolinium has the greatest power[6] of any metal ion to shift the MRI signal of the protons in a water molecule due to its seven unpaired electrons. Because gadolinium is toxic, DTPA is used

to mask its toxicity. Gd(III) has a coordination number of nine[7], while DTPA has eight points of attachment to gadolinium, leaving one available coordination site for a water molecule This is of importance because the ability to shift the MRI signal is a function of the number of water molecules directly attached to gadolinium.[8] An ideal contrast agent would not have as many points of attachment so that more water molecules could coordinate with the gadolinium. The ligand must also be strong enough to form a stable complex with gadolinium.[9]

Fluorescence detectors allow for visualization of metal ions at the molecular level. They also allow for certain metals to be tracked as they move through living cells. Metal ions such as calcium (II) and zinc (II) play an essential role in our biochemical processes.[10,11,12]

Calcium is of special interest because it is known as the universal switch. Calcium turns on enzymes, controls cell division, and releases neurotransmitters to cross synapses. Fluorescence detectors play an important role in the diagnosis and monitoring of Alzheimer's disease. It has been shown that there is a link between a decrease in free cystolic calcium in fibroblasts and the progression of Alzheimer's disease.[13] Currently, the fluorescence detector FURA-2 is used to track this decline.

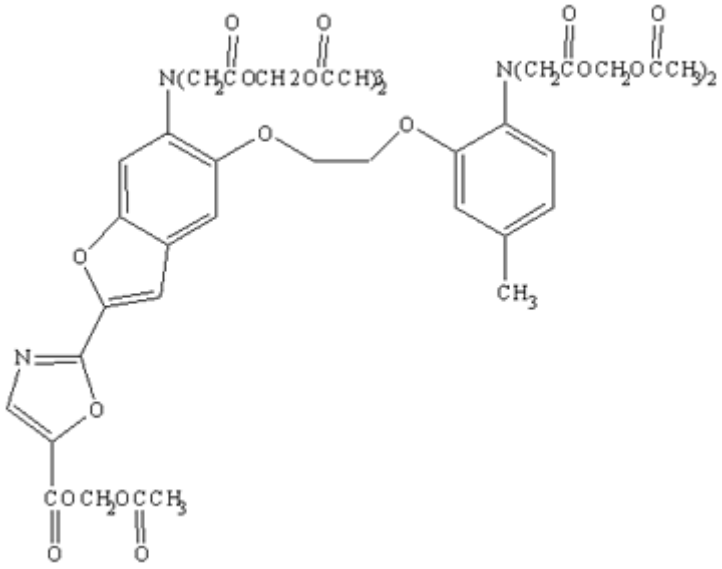

FURA-2

A drawback with FURA-2 is the cost of $150 per 5 milligrams.[14] Therefore, a less expensive alternative with comparable fluorescence and binding properties is desirable.

The majority of zinc present in our body is constricted because it is bound in proteins. Conversely, small amounts of unbound zinc are of interest. It is this unbound zinc that has been shown to possibly play a significant role in neuronal death during seizure as well as neurodegenerative disorders. Currently, Zinquin and other quinoline based detectors are used to track free zinc.[15]

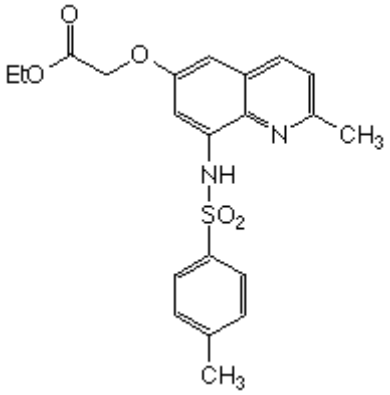

Zinquin

These quinoline based derivatives have flaws in that they can form mixed complexes sensing only partially coordinated zinc.[16]

Lead poisoning affects many people throughout the world.[17] It has been said that at any time in the United States 890,000 children are affected by some type of lead exposure. The most common sources for lead exposure include contaminated soil and lead-based paints. Lead binds strongly to the sulfhydryl groups on proteins and also competes with calcium binding sites.[3] Therefore, when lead is introduced into the body it can cause a wide array of health problems from neurological disorders to death. Treatment of lead poisoning comes in the form of chelation therapy. Chelation therapy involves the introduction of a chelating agent into the body

to form a complex with the undesirable heavy metal (lead) in order to excrete it. Ethylenediamine tetraacetic acid (EDTA) and *meso*-2,3-Dimercaptosuccinic acid (DMSA) are the two most widely used ligands for lead chelation therapy.

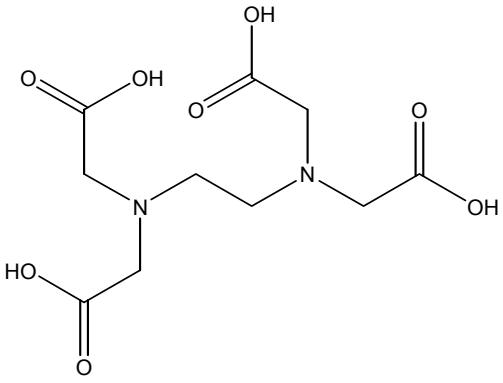

EDTA

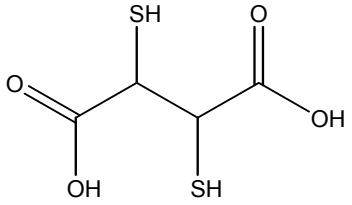

DMSA

EDTA must be given intravenously and requires hospitalization. EDTA has a high affinity for iron as well as lead. In some cases, iron replacement therapy is needed to replenish the iron removed from the body by EDTA. A ligand with a much higher affinity for lead over iron is required to avoid this unwanted side effect. DMSA also has drawbacks such as vomiting, unpleasant taste, and loss of appetite.[18]

When designing a ligand for both medicinal and biological applications as those previously discussed, several factors should be taken into account. The main aspects considered in this study are preorganization,[19,20] chelate ring size,[21] number of donor atoms, and types of donor atoms.[22] Each of these aspects plays an important role in both the selectivity of the ligand for certain metals as well as the thermodynamic stability of the metal-ligand complex formed.

A molecule is said to be more preorganized the more it is constrained as the free ligand to be in the conformation required to bind to its target. Unlike ordinary chemical reactions, where bond strength controls the strength of interaction, preorganized molecules depend primarily on shape to react with a target. Donald Cram won the Nobel Prize in 1987 for his concept of

preorganization.[19] Preorganization is a dominant principle in biology, where molecular recognition is controlled by shape, and the actual chemical interactions may be very weak, consisting only of hydrogen bonding and van der Waals interactions. Macrocycles and cryptands are examples of preorganized ligands. The cyclic structure of these ligands keep them more nearly in the correct conformation for complexing with certain metal ions. Potassium is shown below forming a complex with both macrocyclic crown ether and a cryptand. Potassium has the right size to fit within the cavity of the ligand.

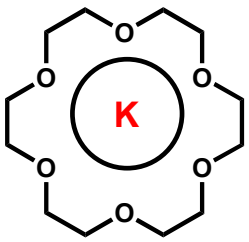

macrocycle (crown ether)

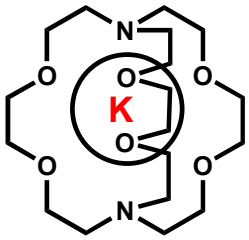

cryptand

The ability of the macrocyclic crown ether and cryptand to form a metal-ion selective thermodynamically stable complex with potassium is also based on chelate ring size. As one can see in the above macrocyle and cryptand a 5-membered chelate ring is formed with potassium. This stabilizes the complex because 5-membered chelate rings are able to fit larger metal ions such as K^+ and Pb^{2+}. Conversely, a 6-membered chelate ring is able to fit smaller metal ions better. This concept is demonstrated below with Pb (II) and Cu (II).

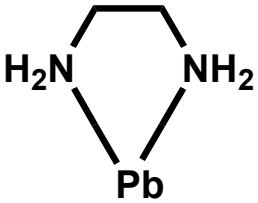

5-membered chelate ring
Pb(II) large
r^+ = 1.19 Å

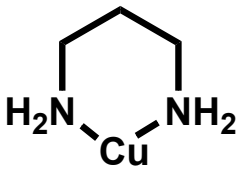

6-membered chelate ring
Cu(II) small
r^+ = 0.57 Å

The smallest metal ion Be^{2+} is comparable in size to a carbon atom, so that it forms a more stable complex in six-membered chelate rings, as does carbon in a cyclohexane ring. In the cyclohexane ring the carbon atoms are equidistant from each other with the hydrogen atoms being staggered.

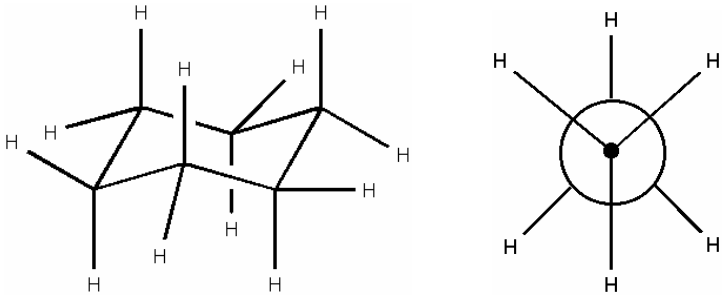

The five-membered carbon ring, cyclopentane, is not very stable because the axial hydrogens eclipse each other. Therefore, when a smaller metal ion is introduced into a 5-membered chelate ring its geometry does not change and it remains sterically unfavorable. However, when a large metal ion is introduced into a 5-membered chelate ring the hydrogen atoms become staggered because of the change in metal-ligand bond length which make the ring sterically favorable.[23]

Donor atoms are points of attachment from a ligand to the metal. Coordination number refers to the number of binding sites on a metal and is what determines the number of donor atoms needed to form a complex with a particular metal. The chelate effect refers to an increase in the formation constant, log K_1, of the metal-ligand complex as the number of chelate rings in a ligand increases. A chelate is a ligand with more than one donor atom. By increasing the number of donor atoms the number of chelate rings formed increases. The number of donor atoms is referred to as denticity. As denticity increases, the formation constant or stability constant of the complex increases. This can be seen in the chart below which shows the formation constants of increasing polyamines complexes with Ni (II). [24]

Polyamine	EN	DIEN	TRIEN	TETREN	PENTEN
denticity, n	2	3	4	5	6
log β_n (NH_3)	5.08	6.85	8.12	8.93	9.08
log K_1 (polyamine)	7.47	10.7	14.4	17.4	19.1

Ionic Strength =	0.5 M
EN	$NH_2CH_2CH_2NH_2$
DIEN	$NH_2(CH_2CH_2NH)_2H$
TRIEN	$NH_2(CH_2CH_2NH)_3H$
TETREN	$NH_2(CH_2CH_2NH)_4H$
PENTEN	$NH_2(CH_2CH_2NH)_5H$
Log $\beta_n(NH_3)$ =	$\log(K_1 \times K_2$ ----- $\times K_n)$

Pearson's Principle of Hard and Soft Acid Bases (HASB)[22,25] indicates which type of metals bind preferentially to which types of donor atoms. A soft base is a donor atom that has high polarizability, low electronegativity, and is easily oxidized. A hard base is a donor atom that has low polarizability, high electronegativity, and is not easily oxidized. A soft acid is an acceptor atom that has a low positive charge, large size and outer electrons that are easily excited. A hard acid is an acceptor atom that has a large positive charge, small size, and lacks easily excited outer electrons. Pearson's HASB Principle states that hard bases form more stable complexes with hard acids and that soft bases form a more stable complex with soft acids. Figure 1 shows a periodic table of metal ions or acceptors and their HASB classification. The trend of decreasing hardness in donor atoms is demonstrated below.

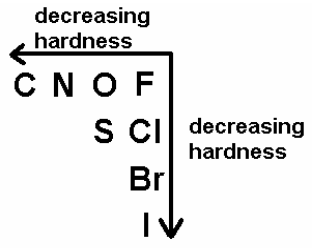

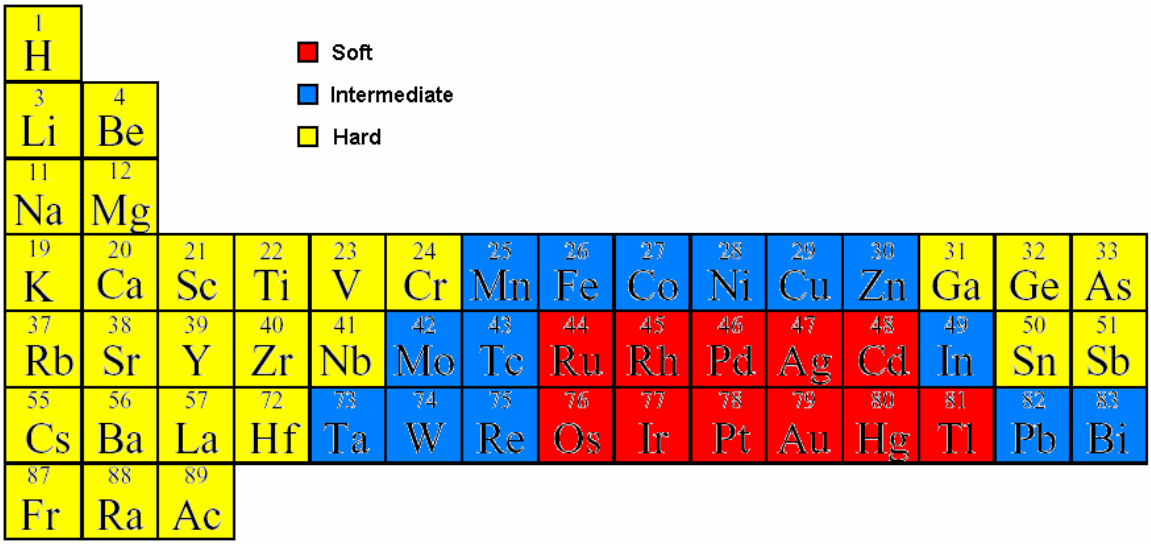

Figure 1: Metal ions classification in HASB Theory according to Pearson.[22,25]

Both 1, 10-phenanthroline-2, 9-dialdoxime (PDOX) and bis-1,10-phenanthroline (DIPHEN) are preorganized hemicycles. These ligands appear promising for use in medicinal and biological applications previously mentioned. Both hemicycles have highly rigid aromatic backbones.

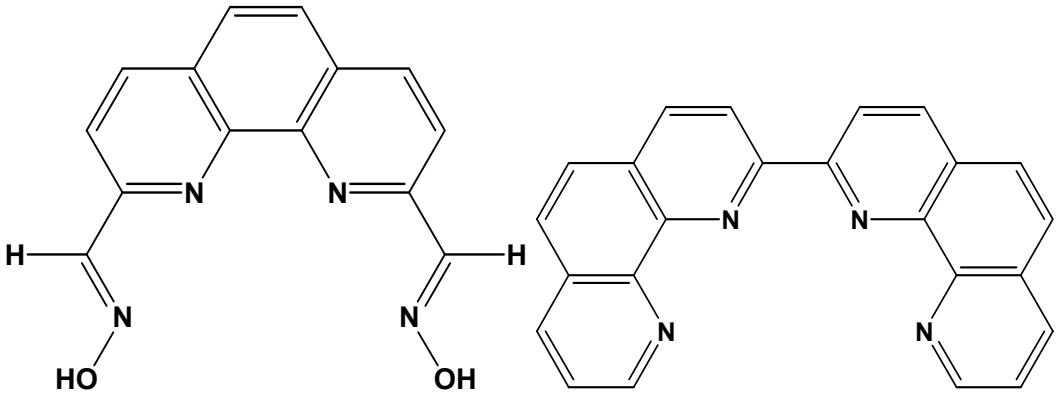

PDOX **DIPHEN**

When DTPA forms a complex with gadolinium, the energy of reorganizing the ligand into the conformation required for complexing the metal ion must be overcome. However, both PDOX and DIPHEN do not have to overcome this reorganization energy because they are already in the correct conformation required to bind to gadolinium. Both ligands also have four donor atoms unlike DTPA which has eight. This leaves five points of attachment on gadolinium for water molecules which in turn would require less metal-ligand complex to be used for MRI imaging.

PDOX and DIPHEN also possess chelation enhanced fluorescence or the CHEF Effect.[2] This is an important characteristic for fluorescence detectors because the lone pairs on the nitrogen atoms on each ligand quench fluorescence, so the ligands will not fully fluoresce until they form a complex with a metal. Lead (II) is a large metal having an atomic radius of 1.19Å. PDOX and DIPHEN have 5-membered chelate rings making them ideal for forming a thermodynamically stable complex with lead. The stability constants, LogK_1, of PDOX and

DIPHEN, and fluorescence properties of the complexes of PDOX with various metal ions are the subject of this research.

METHODS

All chemicals and reagents were analytical grade and purchased commercially. All aqueous solutions of free ligands, metal ions, and metal-ligand complexes were prepared using deionized (DI) water. All percentages are by volume.

All products of organic synthesis were characterized using NMR and FT-IR analysis. All NMR spectra were obtained using a Bruker 400 MHz spectrometer and were referenced using DMSO-d_6. A Polaris IR-10410 FT-IR instrument (Matson, Inc.) with WinFIRST software was used to obtain infrared absorption spectra. All samples for FT-IR analysis were analyzed as KBr Pellets.

UV/Vis absorbance spectra for all aqueous ligand and metal-ligand titrations were carried out using a double beam Cary 1E UV/Vis spectrophotometer (Varian, Inc.) with WinUV Version 2.00(25) software. A quartz 1.0 cm flow cell, fitted with a variable flow peristaltic pump, was used to induce mixing of the aqueous metal-ligand solution after each addition of acid or base in the titration was made. Mixing was further enhanced by stirring the solution using a stir bar and stir plate under the titration vessel. A diagram of the flow cell apparatus can be seen in Figure 2. The aqueous metal-ligand solutions were allowed to equilibrate for 7 minutes for each titrant addition. Absorbance scans were taken between 190 nm to 350 nm at a rate of 600.00 nm/min. All absorbance spectra were referenced using a 1.0 cm quartz cell filled with DI water which was placed in the path of the reference beam.

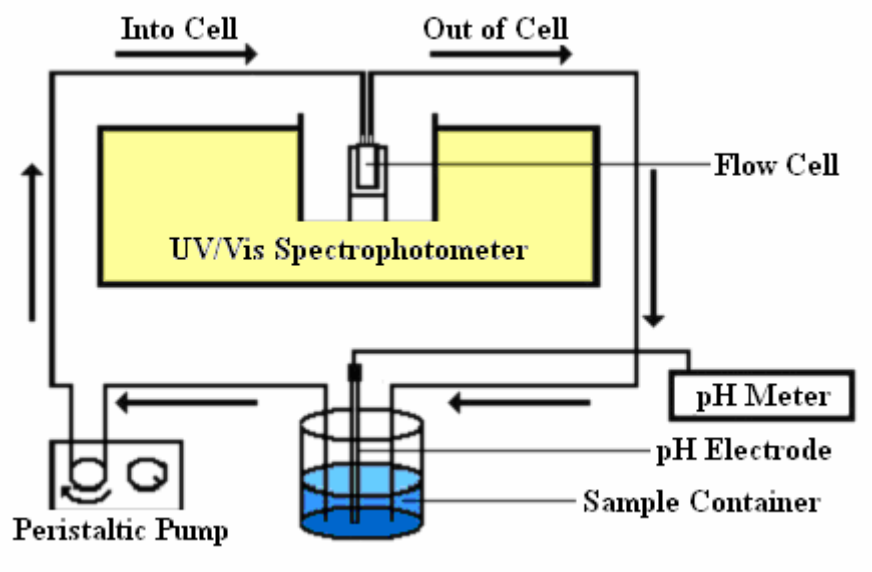

Figure 2: Scheme of the flow cell apparatus used in titration experiments.

All pH values for titration experiments were recorded using a SympHony SR601IC pH meter (VWR Scientific, Inc.). The pH meter was calibrated daily using pH 4.01, 7.00, and 10.00 buffer solutions. All aqueous metal-ligand titration experiments were carried out at a constant temperature of 25.0±0.1˚C controlled by a VWR temperature controller, and the ionic strength was constant using 0.1 *M* $NaClO_4$.

Fluorescence spectra for both the free ligand and metal-ligand complexes were obtained using a Jobin Yvon SPEX Fluoromax-3 scanning fluorometer equipped with a 150 W Xe arc lamp and a R928P detector. Excitation wavelengths were scanned from 250 to 500 nm at 4 nm intervals and emission wavelengths were scanned from 280 nm to 550 nm at 4 nm intervals. The spectra obtained are known as EEM (excitation and emission) spectra. Processing of scans is performed using FLToolbox 1.19 developed for MATLAB® (Release 11).

Overall Synthesis of PDOX

The synthesis of PDOX was carried out using a literature method[26,27] with various modifications. Figure 3 shows a schematic of the synthesis. All products were characterized using ^{1}H-NMR and FT-IR analysis.

Synthesis of PDALD

A mixture of 3.0 g of 2, 9-dimethyl-1,10-phenanthroline monohydrate (14.40 mmol, Alfa Aesar, 99%), also known as neocuprine, and 7.5 g of selenium dioxide (67.59 mmol, Alfa Aesar, 99+ %) was placed in a 250 mL round-bottom flask. The compounds were then dissolved by the addition of 200 mL of 5% DI water/95% p-dioxane (Alfa Aesar, 99+ %). The mixture was then heated to 101 ˚C in a wax bath while stirring, and

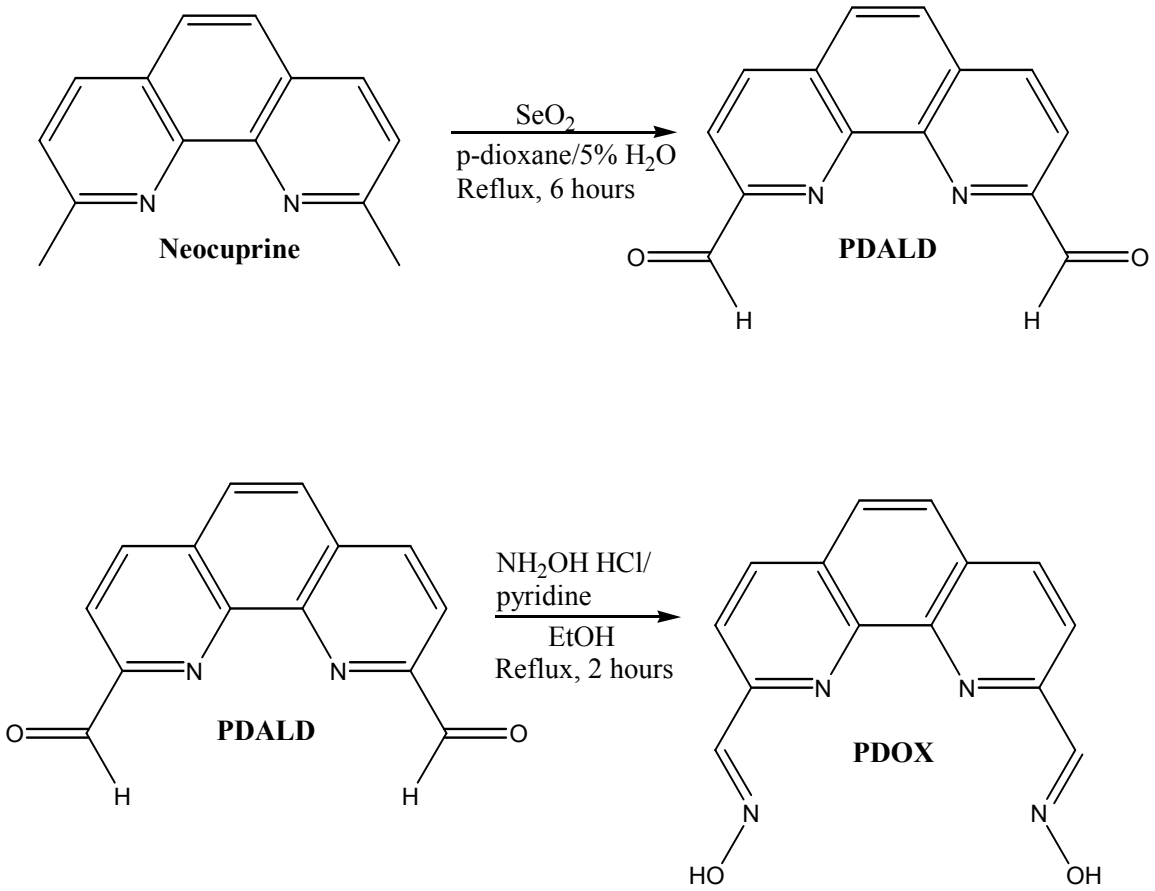

Figure 3: Scheme showing the synthesis of PDOX.[26,27]

allowed to reflux for 6 hours. The hot solution was then filtered through filter paper (Whatman) by vacuum filtration and refrigerated overnight. The yellow-orange precipitate formed in the solution was allowed to warm to room temperature and the impure product was isolated by vacuum filtration. The product was then placed in a 500 mL round-bottom flask and recrystallized in 300 mL of tetrahydrofuran (Burdick & Jackson, 99+%). The yellow crystals of the product were then isolated by vacuum filtration. Selenium dioxide was still visible in the product, indicating that it was impure 1,10-phenanthroline-2, 9-dicarboxylic acid (PDALD), yielding 0.8 g (3.39 mmol, 24 %).

Purification of PDALD

Column chromatography was utilized to purify PDALD. A gravity column was prepared with silica gel (100-200 mesh) and loaded with 0.28 g of impure PDALD (1.19 mmol). The column was then eluted with 9:1 methylene chloride: methanol (Burdick & Jackson, 99+ %). Seventeen 5 mL fractions were collected and analyzed via TLC with a solvent system of 9:1 methylene chloride: methanol. Fractions 4 through 6 were combined (R_f =0.394) and dried under vacuum to give a white powder yielding 0.124 g (0.525 mmol, 43.8 % column purified) of pure PDALD.

Synthesis of PDOX

90 mg (0.38 mmol) of purified PDALD was placed in a 25 mL round-bottom flask and dissolved in 2.25 mL of ethanol (Alfa Aesar, 95 %), and stirred at 60 ˚C for 10 minutes in a water bath. After 10 minutes 140 mg of hydroxylamine hydrochloride (2.01 mmol, Alfa Aesar, 99 %) was added, as well as 6.75 mL of ethanol. The solution was allowed to stir for an additional 5 minutes. An additional 5 mg of hydroxylamine hydrochloride (0.072 mmol) was added to the solution and a yellow precipitate was observed. The temperature of the reaction

was gradually increased to 80 ˚C and allowed to remain there for a period of 20 minutes. After 20 minutes the temperature of the reaction was gradually increased to 95 ˚C, and 369 μL of pyridine (Acros, 99+ %) was added to the reaction flask. The reaction was then allowed to reflux at 95 ˚C for 2 hours. After 2 hours the reaction was cooled to room temperature, the product was isolated by vacuum filtration, and washed with cold DI water. The result was 85.4 mg (0.32 mmol, 84 %) of pure PDOX. The 85.4 mg of pure product obtained represented 9 % overall yield for both synthetic steps and purification of the product.

UV-Vis spectrophotometric titrations involving PDOX

Acid-base titrations of aqueous PDOX and metal-PDOX solutions were monitored using UV-Vis spectrometry. The following stock solutions were used for these titrations. A stock solution of 1.00×10^{-4} *M* PDOX solution (0.026 g into 1 L of DI water). A stock solution of 0.1 *M* $HClO_4$ (8.62 mL of 11.6 *M*, 70 % Alfa Aesar, in 1 L of DI water). A 1 *M* solution of $NaClO_4$ (61 g, Alfa Aesar, 98.0-102.0 %, into 500 mL of DI water). A stock solution of 0.1 *M* NaOH was made to be used as a titrant (5 mL of 10.00 ± 0.05 *M* NaOH, VWR, into a 500 mL volumetric flask filled to volume with DI water). For all UV-Vis spectrometry experiments a 50 mL solution of 2.00×10^{-5} *M* PDOX (10 mL, 1.00×10^{-4} M PDOX), 0.01 M $HClO_4$ (5 mL of 0.1 *M* $HClO_4$), and 0.09 *M* $NaClO_4$ (4.5 mL of $NaClO_4$) filled to volume with DI water was used to maintain an ionic strength of 0.1 *M*. This solution will be referred to as the PDOX stock solution at 0.1 *M* ionic strength and was used in all free PDOX and metal-PDOX titrations to be described.

Solution for titration of PDOX

To determine the protonation constants for PDOX a 50.00±0.05 mL aliquot of PDOX stock solution at 0.1 *M* ionic strength was placed in the flow cell apparatus previously described. The solution was then titrated with the 0.1 *M* NaOH stock solution. Absorbance values were recorded at 241 nm, 259 nm, 287 nm, and 313 nm from each spectrum. The pH values were recorded for each titrant addition.

Solution for titration of PDOX with cadmium (II)

A stock solution of 0.003366 *M* Cd $(ClO_4)_2$ was prepared (0.0554 g, Aldrich, in 50 mL of DI water) for use in the titration. A 50.00±0.05 mL solution of 2×10^{-5} *M* PDOX stock solution at 0.1 *M* ionic strength and 2×10^{-5} M $Cd(ClO_4)_2$ (297 µL of 0.003366 M $Cd(ClO_4)_2$) was placed in the flow cell apparatus previously described. The solution was then titrated with the 0.1 *M* NaOH stock solution. Absorbance values were recorded at 241 nm, 259 nm, 287 nm, and 313 nm from each spectrum. The pH values were recorded for each titrant addition.

Solution for titration of PDOX with calcium (II)

A 50.00±0.05 mL solution of 2×10^{-5} *M* PDOX stock solution at 0.1 *M* ionic strength and 0.0333 *M* $Ca(ClO_4)_2$ (0.530 g of $Ca(ClO_4)_2\bullet4H_2O$ in 50 mL DI water, Aldrich 99 %) was prepared and placed in the flow cell apparatus. The solution was then titrated with the 0.1 *M* NaOH stock solution. Absorbance values were recorded at 241 nm, 259 nm, 287 nm, and 313 nm from each spectrum. The pH values were recorded for each titrant addition.

Solution for titration of PDOX with copper (II)

A stock solution of 0.03320 *M* $Cu(ClO_4)_2$ (0.620 g, Aldrich 98 %, in 50 mL of DI water) was prepared. A 50.00±0.05 mL solution of 2×10^{-5} *M* PDOX stock solution at 0.1 *M* ionic strength and 2×10^{-5} *M* $Cu(ClO_4)_2$ (30 µL of 0.03320 M $Cu(ClO_4)_2$) was placed in the flow cell apparatus previously described. The solution was then titrated with the 0.1 *M* NaOH stock solution. Absorbance values were recorded at 241 nm, 259 nm, 287 nm, and 313 nm from each spectrum. The pH values were recorded for each titrant addition.

Solution for titration of PDOX with gadolinium (III)

A stock solution of 0.0278 *M* $Gd(NO_3)_3$ (0.629 g, Aldrich 99 %, in 50 mL of DI water) was prepared. A 50.00±0.05 mL solution of 2×10^{-5} *M* PDOX stock solution at 0.1 *M* ionic strength and 2×10^{-5} *M* $Gd(NO_3)_3$ (36 µL of 0.0278 *M* $Gd(NO_3)_3$) was placed in the flow cell apparatus previously described. The solution was then titrated with the 0.1 *M* NaOH stock solution. Absorbance values were recorded at 241 nm, 259 nm, 287 nm, and 313 nm from each spectrum. The pH values were recorded for each titrant addition.

Solution for titration of PDOX with lead (II)

A stock solution of 0.0033 *M* $Pb(ClO_4)_2$ (0.0762 g, Aldrich 97 %, in 50 mL of DI water) was prepared. A 50.00±0.05 mL solution of 2×10^{-5} *M* PDOX stock solution at 0.1 *M* ionic strength and 2×10^{-5} *M* $Pb(ClO_4)_2$ (30 µL of 0.0033 *M* $Pb(ClO_4)_2$) was placed in the flow cell apparatus previously described. The solution was then titrated with the 0.1 *M* NaOH stock solution. Absorbance values were recorded at 241 nm, 259 nm, 287 nm, and 313 nm from each spectrum. The pH values were recorded for each titrant addition.

Solution for titration of PDOX with zinc (II)

A stock solution of 0.0999 *M* $Zn(ClO_4)_2$ (1.86 g, Aldrich, in 50 mL of DI water) was prepared. A 50.00±0.05 mL solution of 2×10^{-5} *M* PDOX stock solution at 0.1 *M* ionic strength and 2×10^{-5} *M* $Zn(ClO_4)_2$ (10 μL of 0.0999 *M* $Zn(ClO_4)_2$) was placed in the flow cell apparatus previously described. The solution was then titrated with the 0.1 *M* NaOH stock solution. Absorbance values were recorded at 241 nm, 259 nm, 287 nm, and 313 nm from each spectrum. The pH values were recorded for each titrant addition.

Solutions for fluorescence studies involving PDOX

A 25 mL stock solution of 1.00×10^{-5} *M* solution of PDOX (0.0665 g PDOX in 25 mL DI water) was prepared and used for all fluorescence studies.

Solution for fluorescence of PDOX

A 1.00×10^{-6} *M* solution of PDOX (500 μL of 1.00×10^{-5} *M* PDOX in 5 mL of DI water) was used to determine the intensity of fluorescence of the free ligand. The intensity was recorded at an excitation wavelength of 275 nm and an emissions wavelength of 415 nm.

Solution for fluorescence of the calcium-PDOX complex

A 5 mL solution of 1.00×10^{-6} *M* PDOX (500 μL of 1.00×10^{-5} *M* PDOX) and 1×10^{-6} *M* $Ca(ClO_4)_2$ (15 μL of 0.000333 *M* $Ca(ClO_4)_2$) was used to determine the intensity of fluorescence of the calcium-PDOX complex. The intensity was recorded at an excitation wavelength of 275 nm and an emissions wavelength of 415 nm.

Solution for fluorescence of the cadmium-PDOX complex

A 5 mL solution of 1.00×10^{-6} *M* PDOX (500 µL of 1.00×10^{-5} *M* PDOX) and 1×10^{-6} *M* $Cd(NO_3)_2$ (5 µL of 0.01016 *M* $Cd(NO_3)_2$) was used to determine the intensity of fluorescence of the cadmium-PDOX complex. The intensity was recorded at an excitation wavelength of 275 nm and an emissions wavelength of 415 nm.

Solution for fluorescence of the mercury-PDOX complex

A stock solution of 8.31×10^{-4} M $Hg(ClO_4)_2$ (0.0083 g $Hg(ClO_4)_2$ in 25 mL of DI water) was prepared. A 5 mL solution of 1.00×10^{-6} *M* PDOX (500 µL of 1.00×10^{-5} *M* PDOX) and 1×10^{-6} *M* $Hg(ClO_4)_2$ (6 µL of 8.31×10^{-4} *M* $Hg(ClO_4)_2$) was used to determine the intensity of fluorescence of the mercury-PDOX complex. The intensity was recorded at an excitation wavelength of 275 nm and an emissions wavelength of 415 nm.

Solution for fluorescence of the lead-PDOX complex

A 5 mL solution of 1.00×10^{-6} *M* PDOX (500 µL of 1.00×10^{-5} *M* PDOX) and 1×10^{-6} *M* $Pb(ClO_4)_2$ (15 µL of 0.000316 M $Pb(ClO_4)_2$) was used to determine the intensity of fluorescence of the lead-PDOX complex. The intensity was recorded at an excitation wavelength of 275 nm and an emissions wavelength of 415 nm.

Solution for fluorescence of the zinc-PDOX complex

A 5 mL solution of 1.00×10^{-6} *M* PDOX (500 µL of 1.00×10^{-5} *M* PDOX) and 1×10^{-6} *M* $Zn(ClO_4)_2$ (15 µL of 0.000333 M $Zn(ClO_4)_2$) was used to determine the intensity of

fluorescence of the zinc complex. The intensity was recorded at an excitation wavelength of 275 nm and an emissions wavelength of 415 nm.

UV-Vis spectrometry titrations involving DIPHEN

Acid-base titrations of aqueous DIPHEN and metal-DIPHEN solutions were monitored using UV-Vis spectrometry. The following stock solutions were used for these titrations. A 1 L solution of 6.425×10^{-6} *M* DIPHEN (0.0023 g DIPHEN in 500 mL DI water) in 0.1 *M* $HClO_4$ (8.6 mL of 11.6 *M* $HClO_4$, 70 % Alfa Aesar, 99.9985 %) was brought to volume with 50 % tetrahydrofuran (THF) (500 mL, Burdick & Jackson, 99+%). This solution was kept at an ionic strength of 0.1, and is referred to as the DIPHEN stock solution. An aqueous 250 mL stock solution of 0.1 *M* NaOH (25 mL of 1 *M* NaOH) in 50 % tetrahydrofuran (125 mL) was used as the titrant for all UV-Vis spectrometry experiments with DIPHEN.

Solution for titration of DIPHEN

A 50.00±0.05 mL aliquot of 6.425×10^{-6} *M* DIPHEN stock solution (in 50% THF) at 0.1 *M* ionic strength was titrated with 0.1 *M* NaOH stock solution in 50 % THF. The solution was placed in the flow cell apparatus previously described and absorbance values were recorded at 227 nm, 255 nm, 279 nm, 296 nm and 312 nm from each spectrum. The pH values were recorded for each titrant addition.

Solution for titration of DIPHEN with calcium (II)

A 50.00±0.05 mL solution of 6.425×10^{-6} *M* DIPHEN stock solution in 50% THF at 0.1 *M* ionic strength, together with 1.642 mL of 1.037 *M* $Ca(ClO_4)_2$ in 50% THF (to give 0.0333 *M*

$Ca(ClO_4)_2$) was placed in the flow cell apparatus previously described. The solution was then titrated with the 0.1 *M* NaOH stock solution in 50 % THF. Absorbance values were recorded at 227 nm, 255 nm, 279 nm, 296 nm and 312 nm from each spectrum. The pH values were recorded for each titrant addition.

Solution for titration of DIPHEN with cadmium (II)

A 50.00±0.05 mL solution of 6.425×10^{-6} *M* DIPHEN stock solution in 50% THF at 0.1 *M* ionic strength, together with 316 μL of 0.001016 *M* $Cd(ClO_4)_2$ (to give 6.425×10^{-6} *M* $Cd(ClO_4)_2$) was placed in the flow cell apparatus previously described. The solution was then titrated with the 0.1 *M* NaOH stock solution in 50 % THF. Absorbance values were recorded at 227 nm, 255 nm, 279 nm, 296 nm and 312 nm from each spectrum. The pH values were recorded for each titrant addition.

Solution for titration of DIPHEN with copper (II)

A 50.00±0.05 mL solution of 6.425×10^{-6} *M* DIPHEN stock solution in 50% THF at 0.1 *M* ionic strength, together with 9.6 μL of 0.0332 *M* $Cu(ClO_4)_2$ (to give 6.425×10^{-6} *M* $Cu(ClO_4)_2$) was placed in the flow cell apparatus previously described. The solution was then titrated with the 0.1 *M* NaOH stock solution in 50 % THF. Absorbance values were recorded at 227 nm, 255 nm, 279 nm, 296 nm and 312 nm from each spectrum. The pH values were recorded for each titrant addition.

Solution for titration of DIPHEN with gadolinium (III)

A 50.00±0.05 mL solution of 6.425×10^{-6} *M* DIPHEN stock solution in 50% THF at 0.1 *M* ionic strength, together with 9.5 µL of 0.03359 *M* $Gd(NO_3)_3$ (to give 6.425×10^{-6} *M* $Gd(NO_3)_3$) was placed in the flow cell apparatus previously described. The solution was then titrated with the 0.1 *M* NaOH stock solution in 50 % THF. Absorbance values were recorded at 227 nm, 255 nm, 279 nm, 296 nm and 312 nm from each spectrum. The pH values were recorded for each titrant addition.

Solution for titration of DIPHEN with lead (II)

A 50.00±0.05 mL solution of 6.425×10^{-6} *M* DIPHEN stock solution in 50% THF at 0.1 *M* ionic strength, together with 32 µL of 0.0100 *M* $Pb(ClO_4)_2$ (to give 6.425×10^{-6} *M* $Pb(ClO_4)_2$) was placed in the flow cell apparatus previously described. The solution was then titrated with the 0.1 *M* NaOH stock solution in 50 % THF. Absorbance values were recorded at 227 nm, 255 nm, 279 nm, 296 nm and 312 nm from each spectrum. The pH values were recorded for each titrant addition.

Solution for titration of DIPHEN with zinc (II)

A 50.00±0.05 mL solution of 6.425×10^{-6} *M* DIPHEN stock solution in 50% THF at 0.1 *M* ionic strength, together with 160 µL of 2.00×10^{-3} *M* $Zn(ClO_4)_2$ (to give 6.425×10^{-6} *M* $Zn(ClO_4)_2$) was placed in the flow cell apparatus previously described. The solution was then titrated with the 0.1 *M* NaOH stock solution in 50 % THF. Absorbance values were recorded at 227 nm, 255 nm, 279 nm, 296 nm and 312 nm from each spectrum. The pH values were recorded for each titrant addition.

RESULTS AND DISCUSSION

Synthesis of PDOX

The overall yield in the synthesis of 1,10-phenanthroline-2,9-dialdoxime (PDOX) was 9 %. The yield is low due to the inefficiency of the first step in which 2,9-dimethyl-1,10-phenanthroline monohydrate is oxidized to 1,10-phenanthroline-2,9-dicarboxylic acid (PDALD). Selenium dioxide was utilized as the oxidizing reagent resulting in a yield of 24 % of impure PDALD. Therefore, a purification step was needed to obtain pure PDALD. Column chromatography proved to be a time consuming yet useful method of purification. The recovery after purification was 43.8 %. The recovery reported in the literature Chandler *et. al*. was 70 %, however their reported melting point values were lower suggesting an impure product. The melting point range reported in the literature was 231-232 ˚C and the column chromatography purified PDALD has a melting point range of 269-271 ˚C. Both ^{1}H-NMR spectra and ^{13}C-NMR spectra show that pure PDALD was obtained after purification. The ^{1}H-NMR spectra for PDALD can be seen in Figure 4. The aldehyde protons show a peak at 10.36 ppm (H2,9, singlet). The aromatic protons on the phenanthroline ring system can be seen at the following chemical shifts 8.80 (H4,7, doublet), 8.31 (H3,8, doublet), and 8.29 (H5,6, singlet) ppm. Figure 5 shows the ^{13}C-NMR spectra for PDALD. The chemical shifts are as follows for PDALD 194.21 (C1,12), 152.63 (C2,11), 145.68 (C13,14), 138.95 (C4,9), 131.91 (C5,8), 129.72 (C6,7), and 120.64 (C3,10) ppm. Both ^{1}H and ^{13}C NMR spectra correspond closely with the reported values in Chandler, *et al*. A characteristic IR stretch was also observed for the C=O at 1700cm^{-1}. This purified PDALD was then used in the final step to make PDOX. Purified PDALD was reacted with hydroxylamine hydrochloride in the presence of pyridine using a gradient temperature range to produce PDOX. The yield for this step of the synthesis was 84 % with a

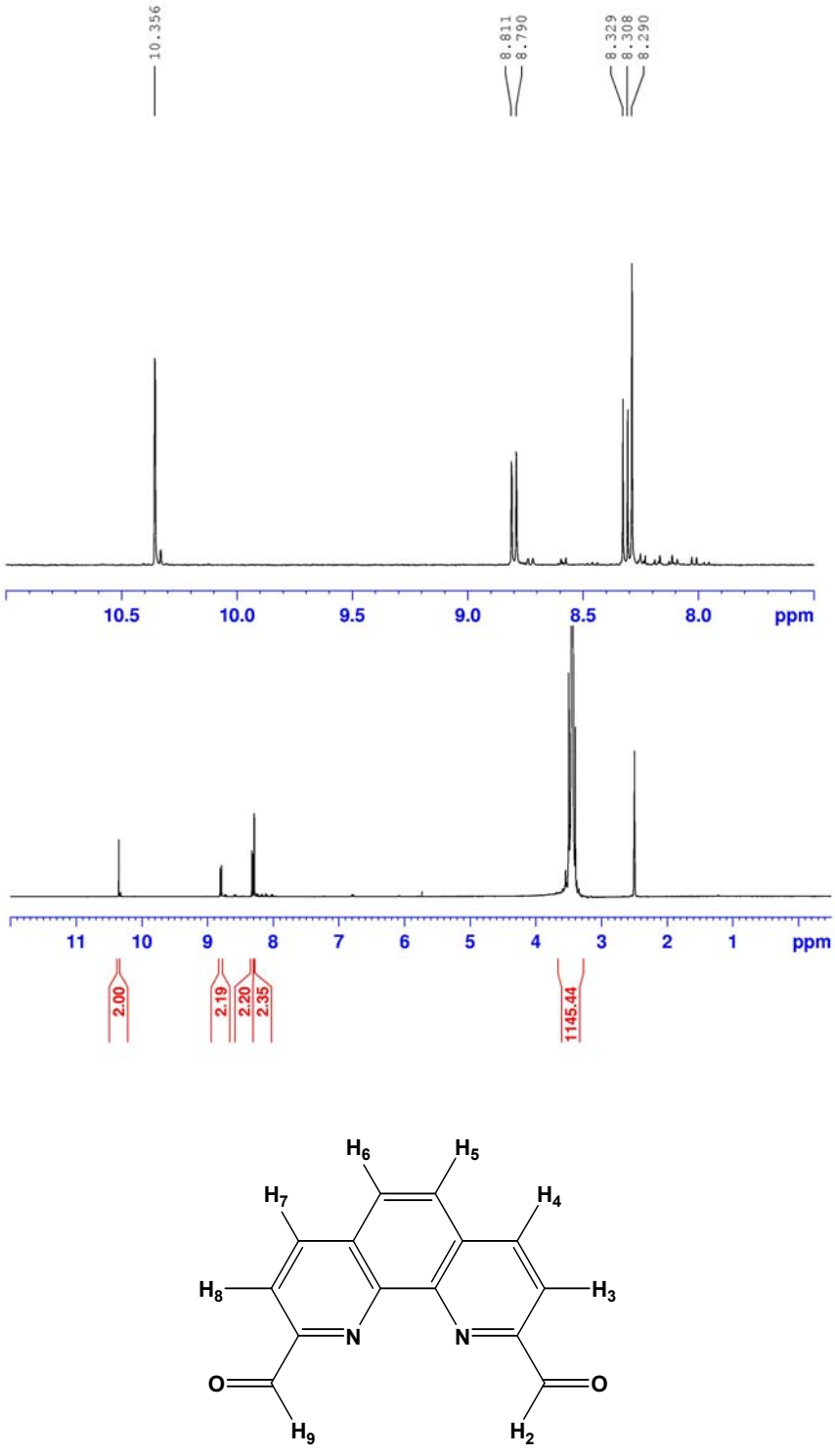

Figure 4: The ^{1}H-NMR spectrum of 1,10-phenanthroline-2,9-dicarboxaldehyde in DMSO-d_6.

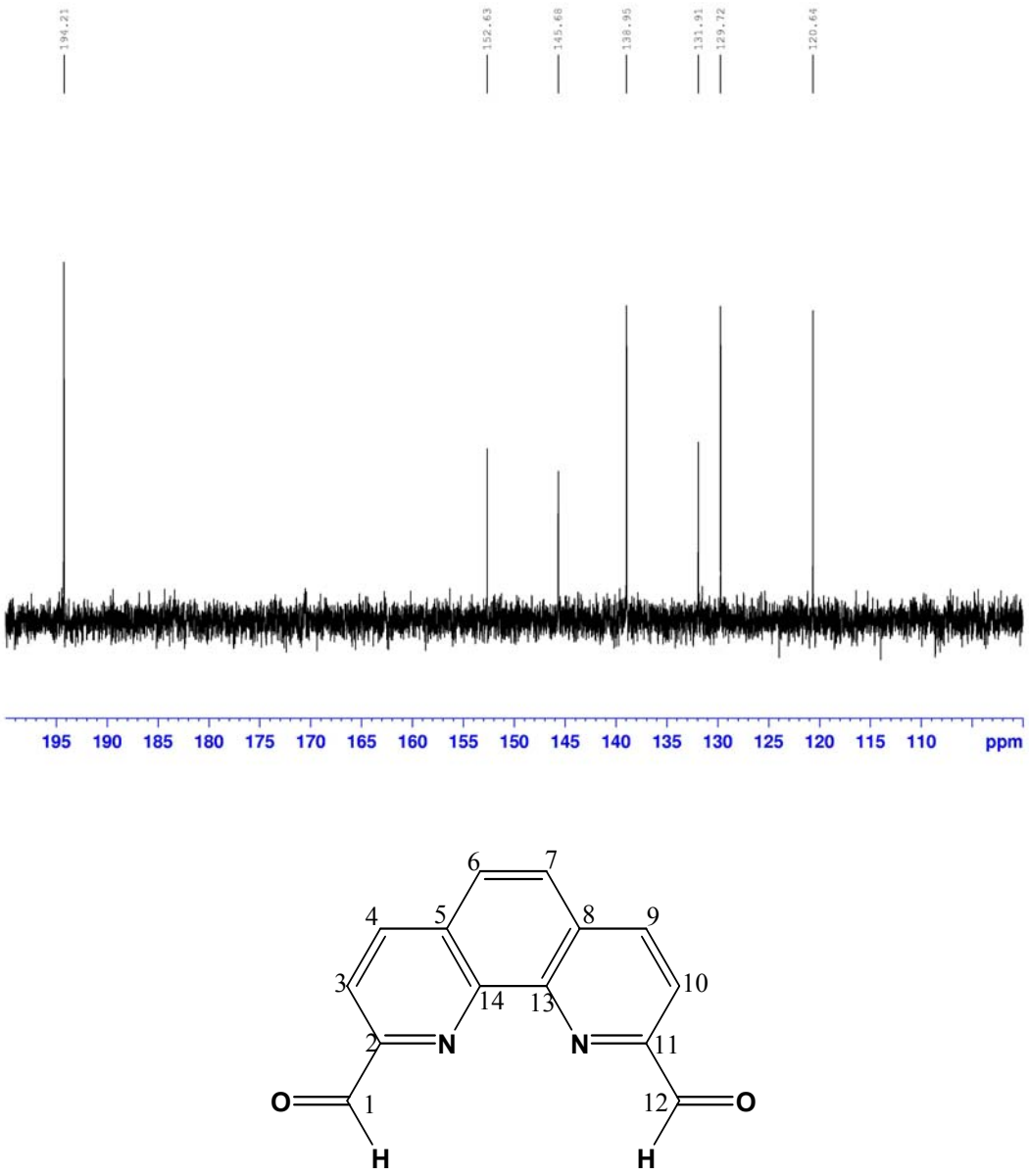

Figure 5: The ^{13}C-NMR spectrum of 1,10-phenanthroline-2,9-dicarboxaldehyde in DMSO-d_6.

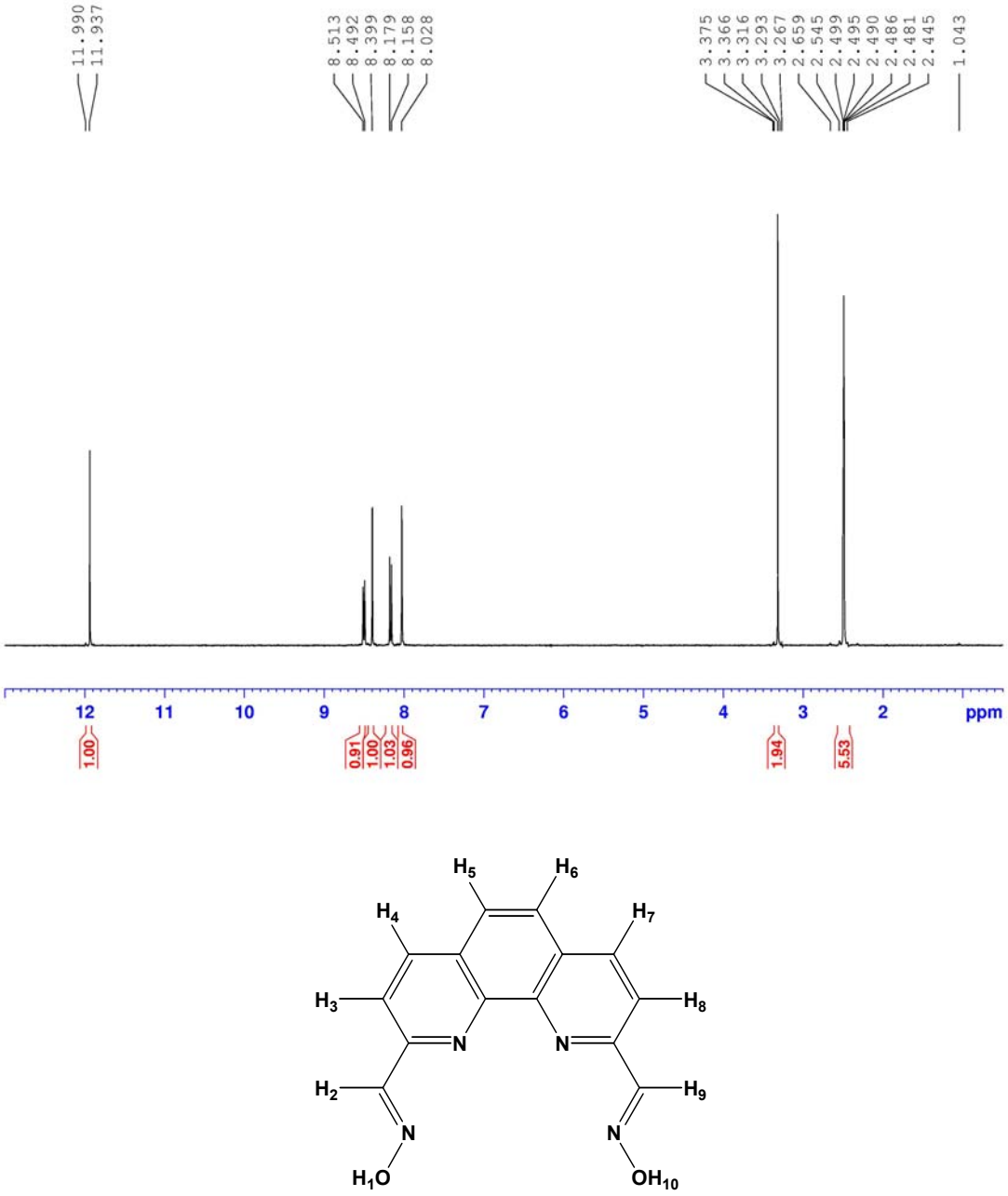

Figure 6: The ^{1}H-NMR spectrum of 1,10-phenanthroline-2,9-dicarboxaldehyde dioxime in DMSO-d_6.

with a melting point range of 269-270 ˚C. Chandler, *et. al*. does not report a yield or melting point range for the synthesis of 1,10-phenanthroline-2,9-dicarbaldehyde dioxime. However, Angeloff, *et. al.* report a yield of 78 % for PDOX and a melting point of 267 ˚C. Therefore, this synthetic step produced a higher yield and purer PDOX than previously reported in the literature. Figure 6 shows the ^{1}H-NMR spectrum of PDOX. The chemical shifts for PDOX are 11.96 (H1,10, singlet), 8.50 (H3,8, doublet), 8.40 (H2,9, singlet), 8.16 (H4,7, doublet), and 8.03 (H5,6, singlet) ppm. A characteristic IR stretch for the C=N was observed at 1614 cm^{-1}.

UV-Vis spectrophotometric titrations Involving PDOX

UV/Vis spectroscopy was used as an analytical tool to determine the stability constants ($\log K_1$) of the metal-PDOX complexes. For each titrant addition of 0.1 *M* NaOH absorbance scans were taken from 190 nm to 350 nm. Absorbance data were taken at selected wavelengths of 241, 259, 287, and 313 nm. Figure 7 shows the absorbance at these wavelengths at varying pH of the free ligand. Peak shifts were seen for these absorbances upon complexation of PDOX with a metal ion.

In order to determine the protonation constants for the ligand, PDOX, titrations were performed at 25.0± 0.1 ˚C at 0.1 *M* ionic strength (0.1 *M* $NaClO_4$). Figure 8 shows absorbance versus wavelength (nm) scans at pH values of approximately 2.00 to 12.00 as an overlay. Absorbance data from 241, 259, 287, and 313 nm were used to generate plots of absorbance versus pH. This data was then used to calculate the protonation constants for PDOX. PDOX as a free ligand has three separate protonation events pK_1, pK_2, and pK_3. These protonation events can be seen in Figure 9. The following calculations were used to determine the actual protonation constant (pK_a,) values for PDOX.

To determine the stability constants from the observed absorbances, it was first necessary to correct each absorbance for dilution using Eq(1).

$$Abs_{Corr} = \frac{Abs \cdot V_{Total}}{V_{initial}} \quad (1)$$

Plots of pH versus Abs_{corr} were constructed for each wavelength selected.

The total ligand concentration, $[L]_{total}$, in solution can be described by Eq(2).

$$L_{Total} = [L] + [LH] + [LH_2] + [LH_3] \quad (2)$$

a.)

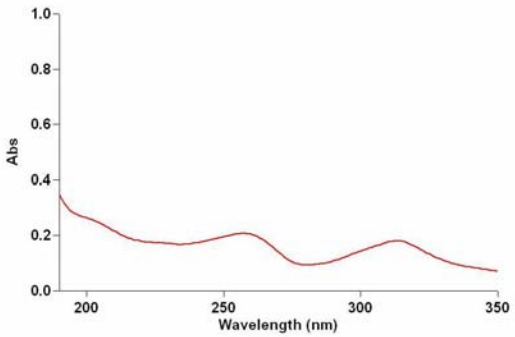

b.)

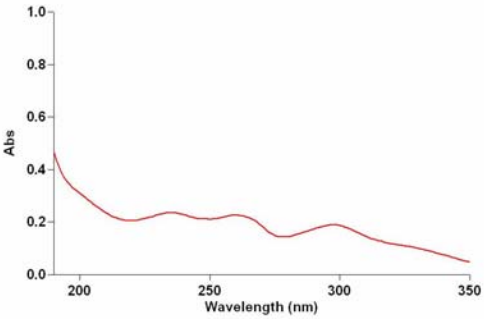

c.)

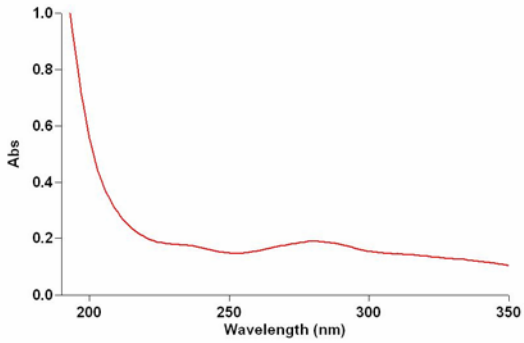

d.)

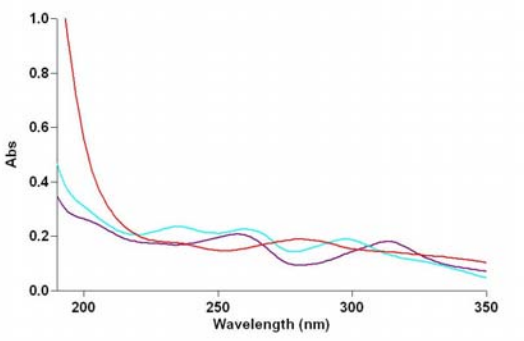

Figure 7: Plots of absorbance versus wavelength (nm) spectra at varying pH from the titration of PDOX at 25.0± ˚C at 0.1 M ionic strength. a.) pH=2.11, b.) pH=5.10 c.) pH=10.15 d.) overlay of pH 2.11, 5.10, and 10.15 spectra.

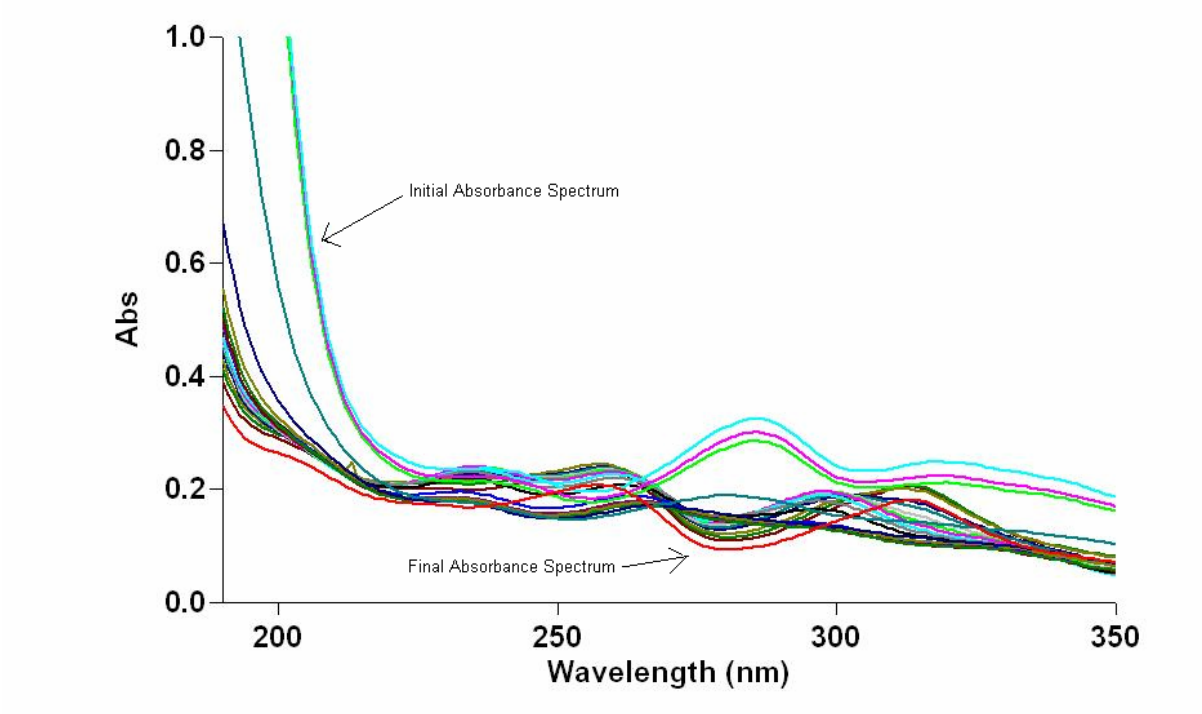

Figure 8: Absorbance versus wavelength (nm) spectra from the titration of PDOX at 25.0±0.1 ˚C for PDOX at 0.1 *M* ionic strength at a pH range of approximately 2.00 to 12.00.

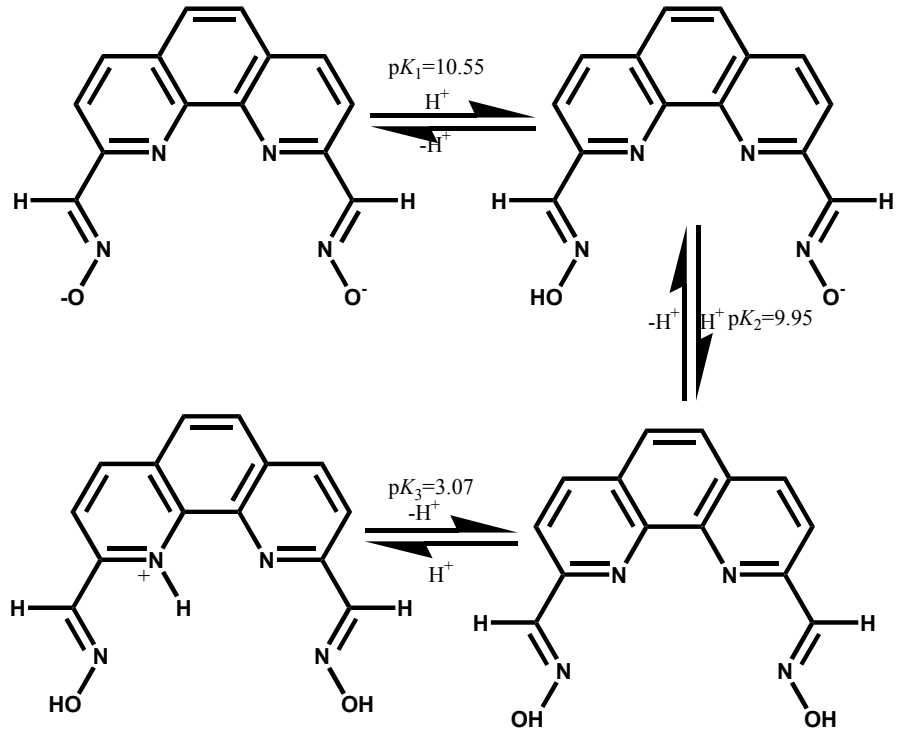

Figure 9: A diagram showing the three protonation events of PDOX

Eq(2) can be rearranged by adding the following protonation constants to get Eq(6). Each Eq(3)-(5) represent a separate protonation event.

$$K_{a1} = \frac{[LH]}{[L][H]} \tag{3}$$

$$K_{a1}K_{a2} = \frac{[LH_2]}{[L][H]^2} \tag{4}$$

$$K_{a1}K_{a2}K_{a3} = \frac{[LH_3]}{[L][H]^3} \tag{5}$$

$$L_{Total} = [L] + K_{a1}[L][H] + K_{a1}K_{a2}[L][H]^2 + K_{a1}K_{a2}K_{a3}[L][H]^3 \tag{6}$$

By dividing out the ligand concentration, [L], Eq(6) can be simplified to Eq(7).

$$\frac{L_{Total}}{[L]} = 1 + K_{a1}[H^+] + K_{a1}K_{a2}[H^+]^2 + K_{a1}K_{a2}K_{a3}[H^+]^3 \tag{7}$$

Theoretical absorbance, Abs(theor), in Eq(8) was calculated by multiplying the concentration of the species present in solution [L, LH, LH_2, and LH_3] by the absorbance of each of these species at a 2 x 10^{-5} *M* concentration, as shown in Eq(7). To simplify Table 1, each term in Eq(7) was described as a function, for example L(func)1 = $K_{a1}[H^+]$.

$$\text{Abs(theor)} = \frac{1 \times [\text{Abs(L)}] + K_{a1}[H^+][\text{Abs(LH)}] + K_{a1}K_{a2}[H^+]^2[\text{Abs(LH}_2\text{)}] + K_{a1}K_{a2}K_{a3}[H^+]^3[\text{Abs(LH}_3\text{)}]}{1 + K_{a1}[H^+] + K_{a1}K_{a2}[H^+]^2 + K_{a1}K_{a2}K_{a3}[H^+]^3} \tag{8}$$

Abs(L) is the absorbance where only unprotonated ligand exists in the sample solution. Abs(LH), Abs(LH_2), and Abs(LH_3) describe the absorbances of each species present at the equilibrium.

Plots of pH versus corrected absorbance were fitted with plots of pH versus Abs(theor) using the 'SOLVER' module of EXCEL at each wavelength selected. This gave the pK_a values seen in Figure 9 with a minimum standard deviation.

Table 1: EXCEL spreadsheet for free ligand used to calculate protonation events.

313 nm	pK1	10.545183
	pK2	9.9451829
	pK3	3.0701146
	Ainf	0.3324883
	A(1)	0.0585997
	A(2)	0.0594774
	A(3)	0.1472985

V(add)	Total Vadd	pH	241	259	287	313	313 corr	L(func)1	L(func)2	L(func)3	L(func)4	A(theor)
0	0	2.05	0.12	0.15	0.05	0.1	0.1185	3E+08	2E+16	3E+17	3E+17	0.1396
0.9	0.9	2.15	0.14	0.17	0.06	0.1	0.138	2E+08	2E+16	1E+17	1E+17	0.1379
0.9	1.8	2.28	0.15	0.18	0.07	0.1	0.137	2E+08	9E+15	5E+16	6E+16	0.135
0.9	2.7	2.74	0.16	0.18	0.08	0.1	0.1208	6E+07	1E+15	2E+15	3E+15	0.1193
0.3	3	2.91	0.16	0.18	0.09	0.1	0.1104	4E+07	5E+14	7E+14	1E+15	0.1114
0.25	3.25	3.11	0.16	0.17	0.09	0.1	0.0983	3E+07	2E+14	2E+14	4E+14	0.1014
0.15	3.4	3.29	0.16	0.17	0.1	0.1	0.0907	2E+07	8E+13	5E+13	1E+14	0.0925
0.08	3.48	3.43	0.16	0.17	0.1	0.1	0.084	1E+07	4E+13	2E+13	6E+13	0.0862
0.12	3.6	3.92	0.16	0.16	0.1	0.1	0.0719	4E+06	4E+12	6E+11	5E+12	0.0703
0.02	3.62	4.37	0.16	0.16	0.11	0.1	0.0715	1E+06	6E+11	3E+10	6E+11	0.0637
0.02	3.64	4.59	0.16	0.16	0.11	0.1	0.0654	901951	2E+11	6E+09	2E+11	0.0621
0.02	3.66	5.03	0.16	0.16	0.11	0.1	0.0627	327479	3E+10	3E+08	3E+10	0.0604
0.02	3.68	5.53	0.16	0.16	0.11	0.1	0.0609	103558	3E+09	9E+06	3E+09	0.0598
0.02	3.7	6.5	0.15	0.15	0.11	0.1	0.0569	11096	3E+07	11494	3E+07	0.0595
0.01	3.71	7.04	0.15	0.15	0.11	0.1	0.0543	3200.2	3E+06	275.73	3E+06	0.0595
0.01	3.72	7.8	0.15	0.14	0.11	0.1	0.0528	556.14	77690	1.447	78249	0.0595
0.01	3.73	7.93	0.15	0.14	0.11	0.1	0.0532	412.27	42694	0.5895	43108	0.0595
0.02	3.75	8.39	0.15	0.14	0.11	0.1	0.0555	142.95	5132.9	0.0246	5276.9	0.0595
0.02	3.77	8.61	0.15	0.14	0.11	0.1	0.0577	86.136	1863.7	0.0054	1950.8	0.0596
0.03	3.8	8.89	0.15	0.14	0.11	0.1	0.0614	45.205	513.29	0.0008	559.5	0.0599
0.05	3.85	9.23	0.15	0.14	0.11	0.1	0.069	20.663	107.24	7E-05	128.9	0.0615
0.12	3.97	9.67	0.15	0.13	0.12	0.1	0.086	7.5021	14.137	4E-06	22.639	0.0712
0.12	4.09	9.98	0.15	0.12	0.14	0.1	0.1002	3.6744	3.3913	4E-07	8.0657	0.0929
0.08	4.17	10.19	0.16	0.12	0.15	0.1	0.1124	2.2656	1.2893	1E-07	4.5549	0.119
0.1	4.27	10.34	0.17	0.14	0.18	0.1	0.1333	1.6039	0.6462	3E-08	3.2501	0.143
0.1	4.37	10.51	0.19	0.15	0.21	0.2	0.1539	1.0844	0.2954	1E-08	2.3798	0.1738
0.12	4.49	10.57	0.23	0.17	0.26	0.2	0.1919	0.9445	0.2241	7E-09	2.1685	0.185
0.2	4.69	10.76	0.25	0.19	0.31	0.2	0.2224	0.6098	0.0934	2E-09	1.7032	0.2195
0.3	4.99	10.92	0.27	0.2	0.36	0.3	0.2536	0.4219	0.0447	6E-10	1.4666	0.2454
0.4	5.39	11.05	0.29	0.21	0.39	0.3	0.2727	0.3127	0.0246	3E-10	1.3373	0.2634
0.5	5.89	11.23	0.3	0.22	0.41	0.3	0.2875	0.2066	0.0107	7E-11	1.2173	0.2836
0.7	6.59	11.39	0.31	0.22	0.42	0.3	0.2863	0.1429	0.0051	2E-11	1.1481	0.2972

To determine log K_1 for metal ion stability, the procedure described above was performed for each metal-ligand complex at the same wavelengths where the presence of the metal ion affects the protonation events observed in two ways. In the first instance, protonation of the ligand now involves displacement of the metal ion by protons:

$$ML + H^+ \rightarrow M + LH \quad (9)$$

In the simple case above, where one proton can be attached to the ligand, one can calculate log K_1 for the complex (ML) as follows. In the case of no metal ion present, a protonation is evidenced by an inflexion of absorbance versus pH. The midpoint of the inflection gives us the pK_a. In the presence of the metal ion, if a complex is formed, an inflection in the absorbance versus pH curve is observed, but now at lower pH. This protonation event corresponds to equation 9. From the position of the midpoint of the inflexion corresponding to equation 9, one can calculate a reaction constant:

$$K_{react} = \frac{[LH][M]}{[ML][H^+]} \quad (10)$$

In equation 10, $[H^+]$ is the proton concentration at pH_{50}, which is the pH in equation 10 where [LH] = [ML]. In calculating K_{react}, the free metal ion concentration [M] must also be included. Thus, K_{react} equals the free metal ion concentration [M], which at pH_{50} will be 50% of the total metal ion concentration ([ML] = [M]), divided by $[H^+]$ at pH_{50}. K_1 for the metal ion complex now corresponds to the constant K_{react} for equation 10 combined with the protonation constant K_a:

$$K_1 = \frac{K_a}{K_{react}} \quad (11)$$

$$= \frac{[LH]}{[L][H^+]} x \frac{[ML][H^+]}{[LH][M]}$$

$$= \frac{[ML]}{[L][M]} \tag{12}$$

If one has a multiprotic ligand such as PDOX, the logic is the same, except that all three (in the case of PDOX) protonation constants are involved.

$$ML + 3\,H^+ \rightarrow M + LH_3 \tag{13}$$

$$K_{react} = \frac{[LH_3][M]}{[ML][H^+]^3} \tag{14}$$

$$K_1 = \frac{K_{a1} x K_{a2} x K_{a3}}{K_{react}} \tag{15}$$

$$= \frac{[LH_3]}{[L][H^+]^3} x \frac{[ML][H^+]^3}{[LH_3][M]}$$

$$= \frac{[ML]}{[L][M]} \tag{16}$$

The other sources of protonation events for metal-ligand complexes can be protonation events involving hydroxides on the complex, as in

$$MLOH + H^+ \rightarrow ML \tag{17}$$

The complex itself may also be protonated as in

$$ML + H^+ \rightarrow MLH^+ \tag{18}$$

The latter would typically involve addition of a proton to a basic site on the complex, with or without loss of coordination of that site to the metal ion. Protonation constants for these events

are determined but are not relevant in the calculation of stability constants of the ligand with metal ions.

UV-Vis spectrophotometric titrations involving metals with PDOX

The formation constants for each metal ion with PDOX were determined using equations 1-16. Protonation constants of the metal-PDOX complex were determined as well. Then the difference of the pK_a values relative to the free ligand were taken and the negative log of the concentration of the free metal was added to this value, thus giving the logK_1 of the metal-PDOX complex. Several titrations yielded apparent protonation constants that corresponded to equations 17 and 18. These pK_a values were not used in the previously described calculation.

MM calculations using HyperChem5.11 were utilized to determine the ideal metal ion size (Å) to form a complex with PDOX.[28] This was done by calculating the approximate ΔU, which is the increase in steric strain (U) on complex-formation in the reaction shown in Figure 10, using the following equation.

$$\sum(U)_{product} - \sum(U)_{reactant} = \Delta U_{\ complex\ formation} \qquad (19)$$

The model reaction used involved the transfer of a metal from a nonpreorganized analog of PDOX (triethylenetetramine) to the metal-PDOX complex. Figure 11 shows a plot of steric energy (kcal/mol) versus ionic radius of metal ions (Å). The minimum in this curve represents an ideal metal ion size for coordinating with PDOX. The plot showed an energy minimum for PDOX with metal ions of an ionic radius around 1.20 Å. Examples of metal ions of this approximate size are Pb(II) at 1.19 Å and Sr(II) at 1.18 Å. As the ionic radii of the metal ions decrease, the steric energy increases dramatically such

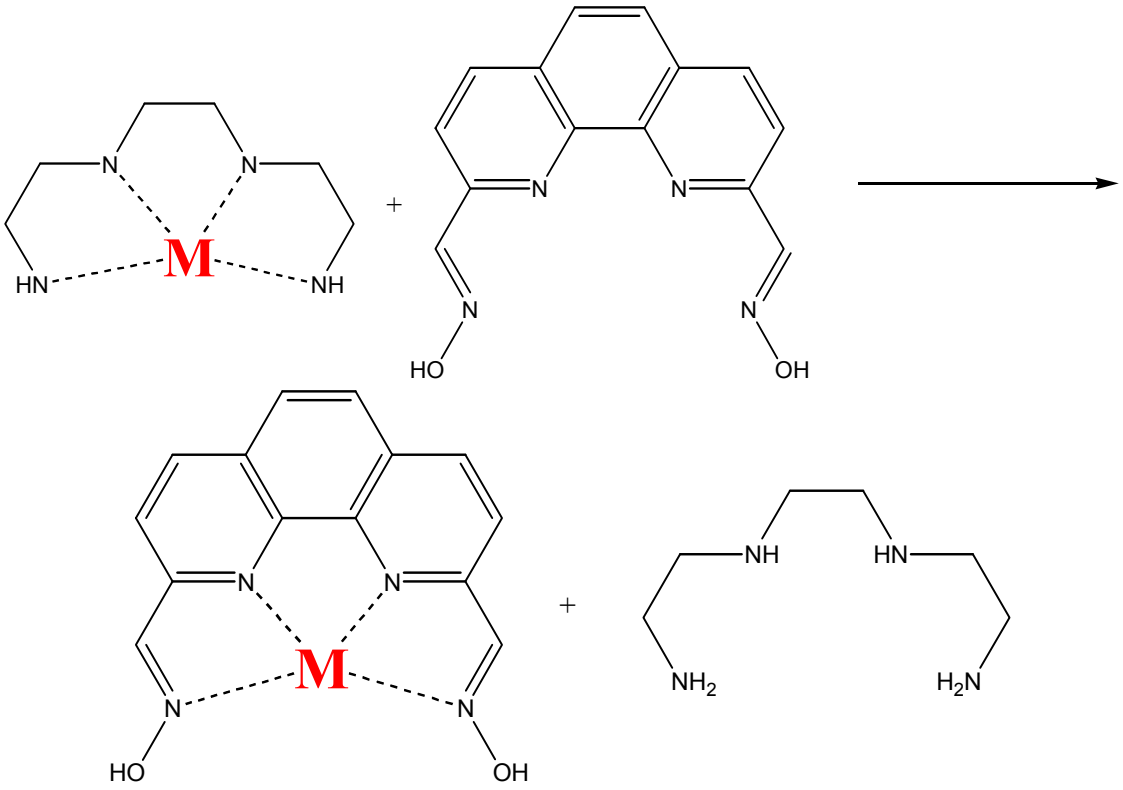

Figure 10: Model reaction used in the calculation of an approximate $\Delta U_{complex\ formation}$ showing the transfer of a metal from a nonpreorganized analog of PDOX (triethyleneteramine) to the metal-PDOX complex.

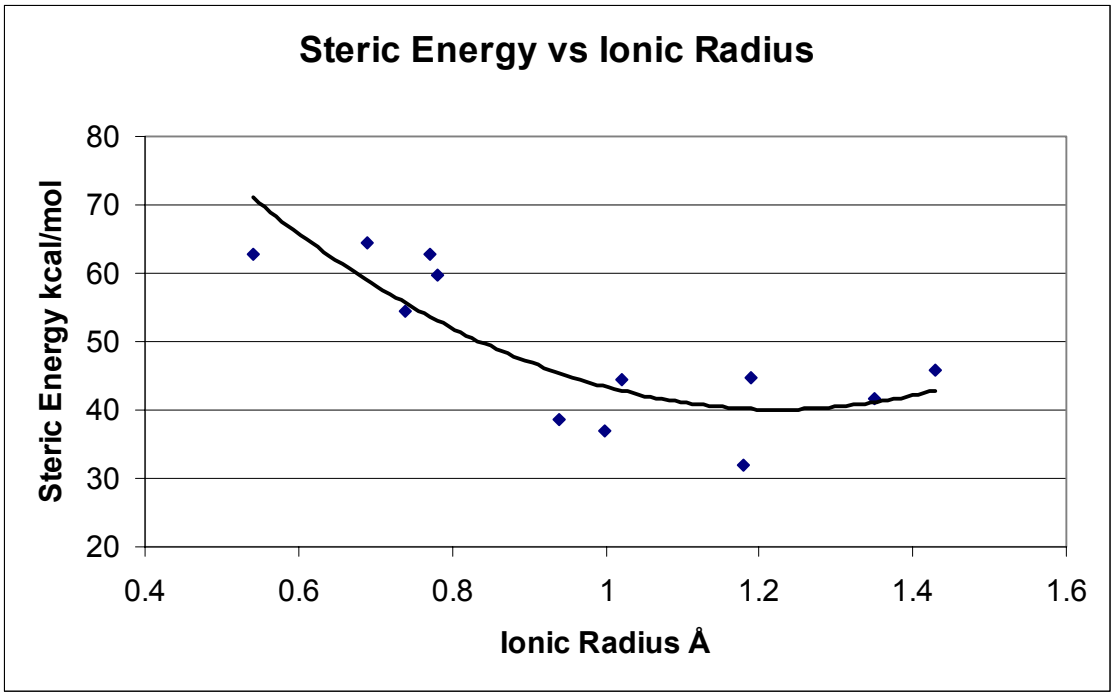

Figure 11: A plot of steric energy (kcal/mol) for PDOX complexes versus ionic radius of metal ions (Å) using HyperChem MM calculations

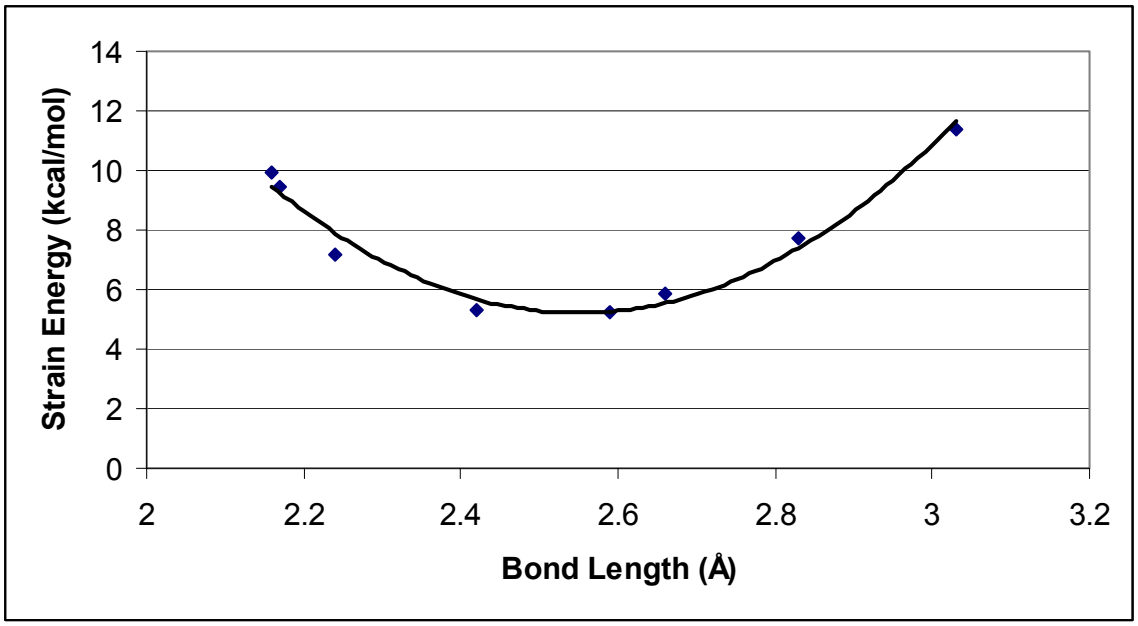

Figure 12: Calculated strain energy (kcal/mol) versus metal nitrogen bond length (Å) for metal-PDOX complexes.

Table 2: Comparison of log K_1 data for metal ions with PDOX and 1,10-phenanthroline.[29]

Metal	Ionic Radius (Å)	log K_1 PDOX(ML)	log K_1 PDOX(MLH)	log K_1 with 1,10-phen(ML)	Δ log $K1$
Ca(II)	0.99		12.05	1.0	
Cd(II)	0.97	9.71		5.4	4.31
Cu(II)	0.57	10.0		9.7	0.3
Gd(III)	0.938	8.75			
La(III)	1.061			2.1	
Pb(II)	1.19	9.43		4.6	4.83
Zn(II)	0.74	8.88		6.4	2.48

as Co(III) at 0.54 Å. As the ionic radii of the metal ions increase, so does the steric energy. This can be seen in the case of Ra(II) at 1.43 Å. Molecular mechanics calculations were also performed for metal ions with PDOX and a plot of energy (kcal/mol) versus metal-nitrogen bond length (Å) was generated, which is illustrated in Figure 12. The stability constants, log K_1, for metals with PDOX calculated from titration experiment complemented the results from the MM calculations. Slight variations were observed which were due to metal ion selectivity for nitrogen donor atoms.

The stability constants determined with metal ions with PDOX from UV-Vis spectroscopy titration experiments can be seen in Table 2. The stability constants are compared to that of 1,10-phenanthroline which is also displayed in Table 2. Most metal-PDOX complexes showed an increase in stability due to the addition of the oxime groups to 1,10-phenanthroline.

PDOX-calcium(II) results

Calcium(II) has an ionic radius of 0.99 Å[30], which is slightly lower than the ideal fit for PDOX at 1.20 Å. However, Ca(II) is classified as a hard metal ion. Therefore, it prefers hard donor atoms.[31] Nitrogen is an intermediate donor atom. This in turn affected the stability of the calcium-PDOX complex. The UV absorbance spectra are shown in Figure 13 for the titration of Ca(II) with PDOX. Also, the corrected absorbance and theoretical absorbance versus pH plots are shown in Figure 14. From the selected wavelengths previously described, apparent pK_a values were seen at 10.8, 8.58, and 4.42. The first pK_a value of 10.8 corresponds to a MLOH complex as seen in equation 17. Thus, a logK_1 for the Metal-Ligand (ML) complex was not able to be calculated. A log$K$ value of 12.05 for the Metal-Ligand-Proton (MLH) complex was

calculated using equation 1-16. The calcium ion was driven out of the complex after the second protonation event of PDOX occurred.

PDOX-cadmium(II) results

The ionic radius of cadmium(II) is 0.97 Å,[30] which again is slightly lower than the ideal fit for PDOX shown by MM calculations. The UV absorbance spectra are shown in Figure 15 for the titration of Cd(II) with PDOX. Also, the corrected absorbance and theoretical absorbance versus pH plots are shown in Figure 16. From the selected wavelengths previously described, apparent pK_a values were seen at 11.34, 9.1, 6.83 and 2.93. The first pK_a value of 10.8 corresponds to a MLOH complex as seen in equation 17. Using equations 1-16, a logK_1 value for the cadmium-PDOX complex was calculated to be 9.71. A Δ logK_1 of 4.31 shows a significant difference in stability between the PDOX complex and the 1,10-phenanthroline complex of Cd(II).

PDOX-copper(II) results

Copper(II) has an ionic radius of 0.57 Å,[30] which is significantly smaller than the desired ionic radius for complexing with PDOX. However, copper is categorized by Pearson as being an intermediate metal ion.[31] These metal ions prefer intermediate donor atoms such as the nitrogen atoms on the oxime functional groups of PDOX. The UV absorbance spectra are shown in Figure 17 for the titration of Cu(II) with PDOX. Also, the corrected absorbance and theoretical absorbance versus pH plots

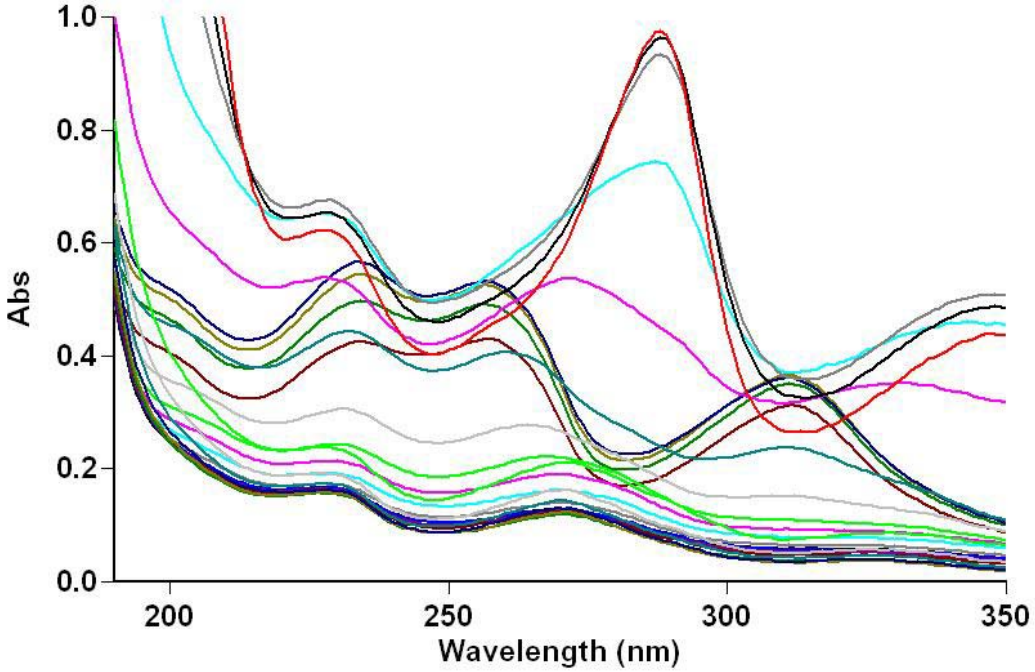

Figure 13: UV absorbance spectra for the titration of Ca(II) (0.0333 *M*) and PDOX ($2x10^{-5}$ *M*) at 25.0±0.1 ˚C, at 0.1 *M* ionic strength, and at a pH range of approximately 2.00 to 12.00.

a.)

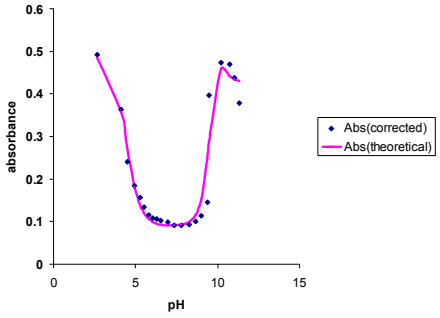

b.)

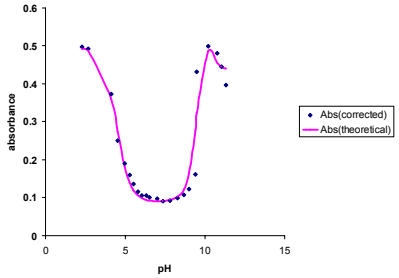

c.)

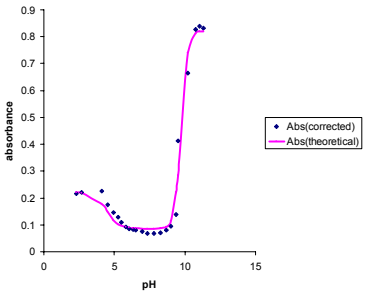

d.)

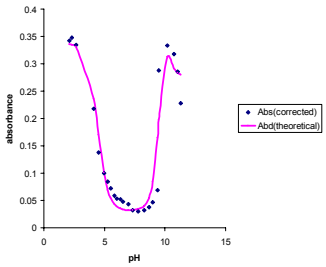

Figure 14: Comparison of corrected absorbance versus theoretical absorbance with respect to pH at wavelengths of a.) 241 nm, b.) 259 nm, c.) 287 nm, and d.) 313 nm for the titration of PDOX with Ca(II).

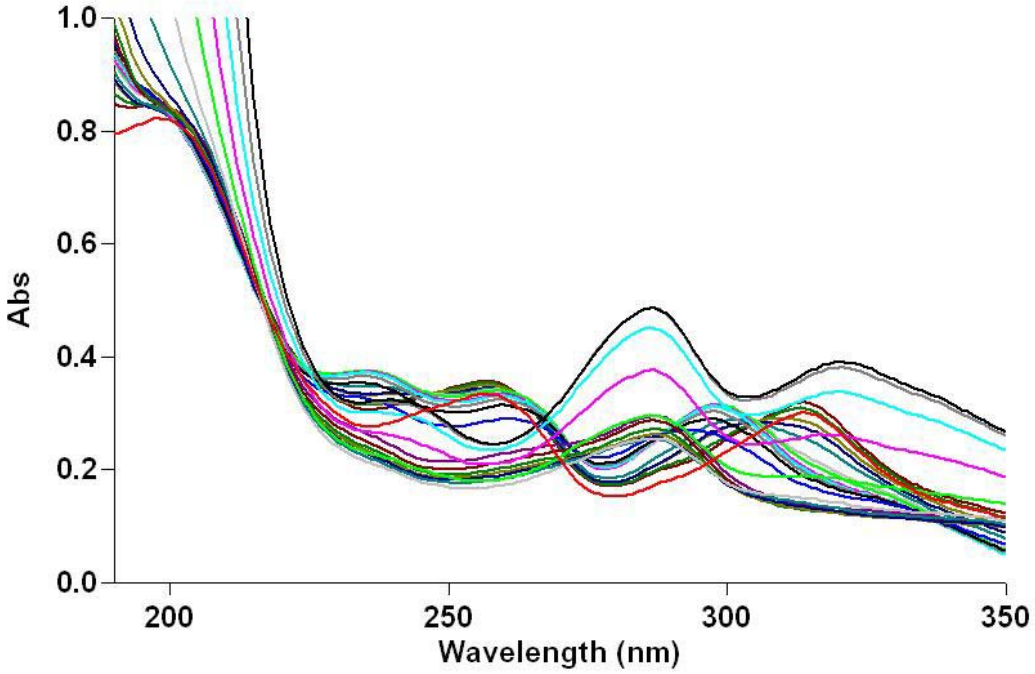

Figure 15: UV absorbance spectra for the titration of Cd(II) ($2x10^{-5}$ *M*) and PDOX ($2x10^{-5}$ *M*) at 25.0±0.1 ˚C, at 0.1 *M* ionic strength, and at a pH range of approximately 2.00 to 12.00.

a.)

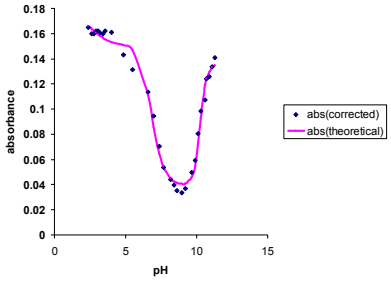

b.)

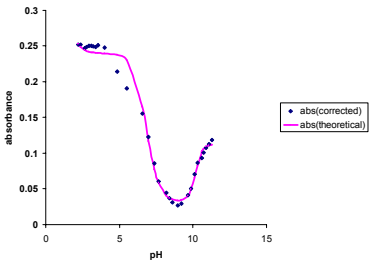

c.)

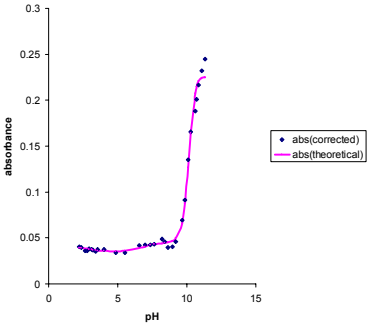

d.)

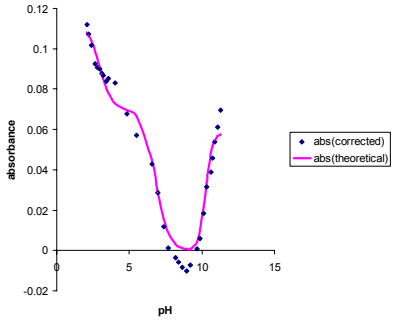

Figure 16: Comparison of corrected absorbance versus theoretical absorbance with respect to pH at wavelengths of a.) 241 nm, b.) 259 nm, c.) 287 nm, and d.) 313 nm for the titration of PDOX with Cd(II).

are shown in Figure 18. From the selected wavelengths previously described, apparent pK_a values were seen at 10.51, 10.29, 4.15 and 4.13. The first pK_a value of 10.51 corresponds to a MLOH complex as seen in equation 17. Using equations 1-16, a logK_1 value for the copper-PDOX complex was calculated to be 10.00. A Δ logK_1 of 0.3 shows a modest difference in stability between the PDOX complex and the 1,10-phenathroline complex of Cu(II).

PDOX-gadolinium(III) results

Gadolinium(III) has an ionic radius of 0.93 Å,[30] which is slightly smaller than the MM calculated ideal ionic radius for PDOX. Gd(III) is classified as hard by Pearson.[31] The UV absorbance spectra are shown in Figure 19 for the titration of Gd(III) with PDOX. Also, the corrected absorbance and theoretical absorbance versus pH plots are shown in Figure 20. From the selected wavelengths previously described, apparent pK_a values were seen at 10.63, 10.40, 6.90 and 2.82. The first pK_a value of 10.63 corresponds to a MLOH complex as seen in equation 17. Using equations 1-16, a logK_1 value for the gadolinium-PDOX complex was calculated to be 8.75. There was no logK_1 reported for 1,10-phenanthroline with Gd(III) to compare PDOX with. In order to approximate the Δ logK_1 a comparison of known logK_1 values with lanthanum(III) can be used due to its similar chemistry with gadolinium(III).[32] This would give an approximate Δ logK_1 of 6.65 when compared to that of 1,10-phenanthroline.

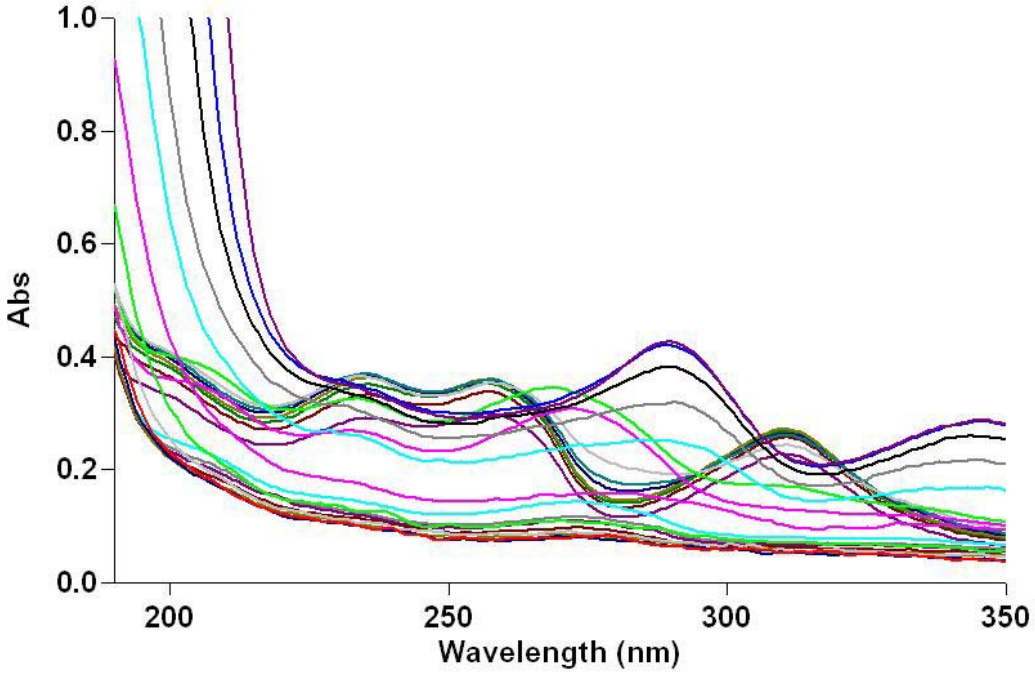

Figure 17: UV absorbance spectra for the titration of Cu(II) ($2x10^{-5}$ *M*) and PDOX ($2x10^{-5}$ *M*) at 25.0±0.1 ˚C, at 0.1 *M* ionic strength, and at a pH range of approximately 2.00 to 12.00.

a.)

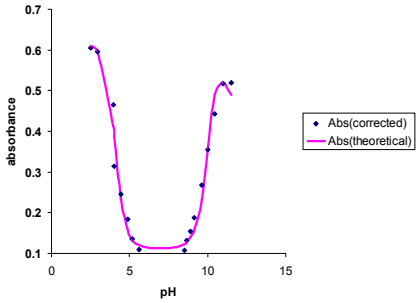

b.)

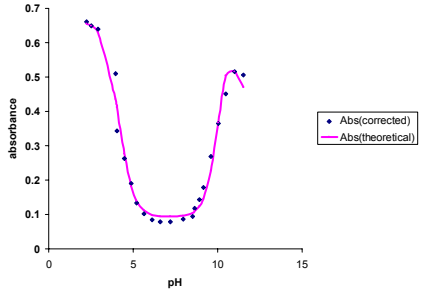

c.)

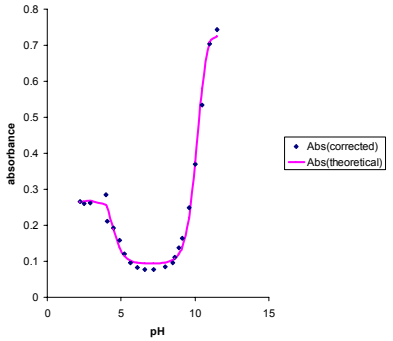

d.)

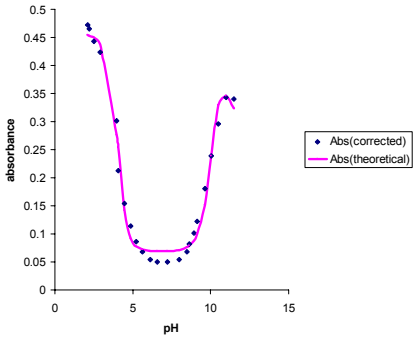

Figure 18: Comparison of corrected absorbance versus theoretical absorbance with respect to pH at wavelengths of a.) 241 nm, b.) 259 nm, c.) 287 nm, and d.) 313 nm for the titration of PDOX with Cu(II).

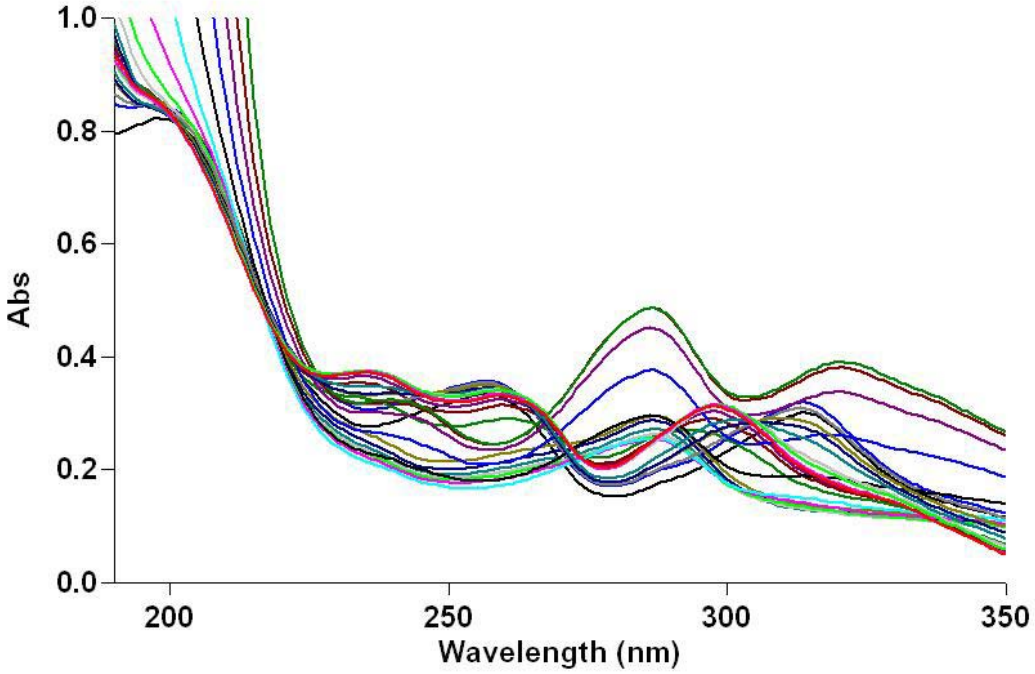

Figure 19: UV absorbance spectra for the titration of Gd(III) ($2x10^{-5}$ *M*) and PDOX ($2x10^{-5}$ *M*) at 25.0±0.1 ˚C, at 0.1 *M* ionic strength, and at a pH range of approximately 2.00 to 12.00.

a.)

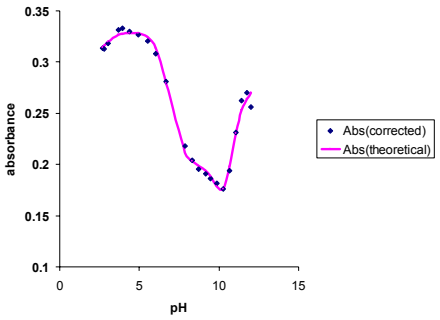

b.)

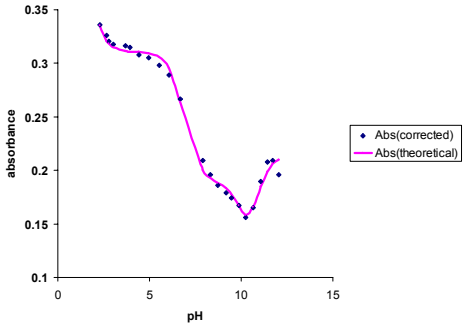

c.)

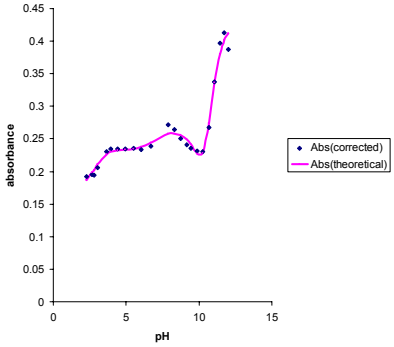

d.)

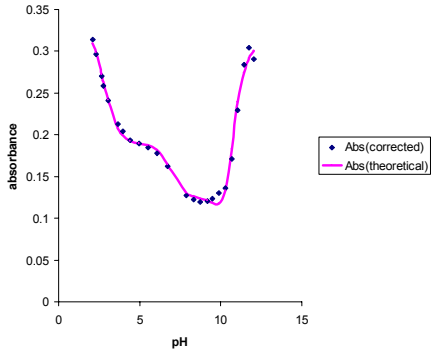

Figure 20: Comparison of corrected absorbance versus theoretical absorbance with respect to pH at wavelengths of a.) 241 nm, b.) 259 nm, c.) 287 nm, and d.) 313 nm for the titration of PDOX with Gd(III).

PDOX-lead(II) results

Lead(II) has an ionic radius of 1.19 Å,[30] which is the desired ionic radius for complexing with PDOX. Lead is classified by Pearson as being an intermediate metal ion.[31] Again, these metal ions prefer intermediate donor atoms such as the nitrogen atoms on the oxime functional groups of PDOX. The corrected absorbance and theoretical absorbance versus pH plots are shown in Figure 21. From the selected wavelengths previously described, apparent pK_a values were seen at 12.21, 10.21, 6.27 and 2.66. The first pK_a value of 12.21 corresponds to a MLOH complex as seen in equation 17. Using equations 1-16, a logK_1 values for the lead-PDOX complex was calculated to be 9.43. A Δ logK_1 of 4.83 shows a quantitative difference in stability between the PDOX complex and the 1,10-phenathroline complex of Pb(II).

PDOX-zinc(II) results

Zinc (II) has an ionic radius of 0.74 Å,[30] which is smaller than the ideal ionic radius for complexing with PDOX. Zinc is also categorized by Pearson as being an intermediate metal ion,[31] which prefers intermediate donor atoms such as the nitrogen atoms on the oxime functional groups of PDOX. The corrected absorbance and theoretical absorbance versus pH plots are shown in Figure 22. From the selected wavelengths previously described, apparent pK_a values were seen at 11.61, 10.55, 6.48 and 2.93. The first pK_a value of 11.61 corresponds to a MLOH complex as seen in equation 17. Using equations 1-16, a logK_1 value for the zinc-PDOX

a.)

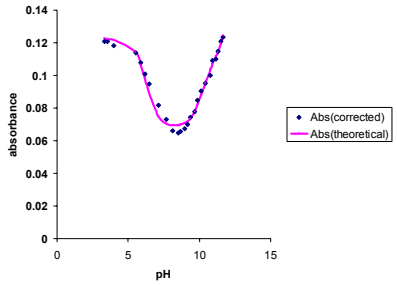

b.)

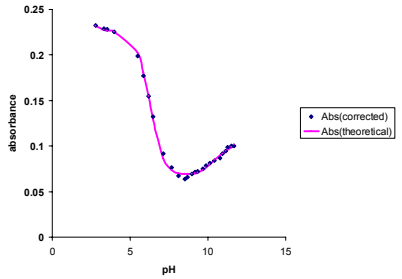

c.)

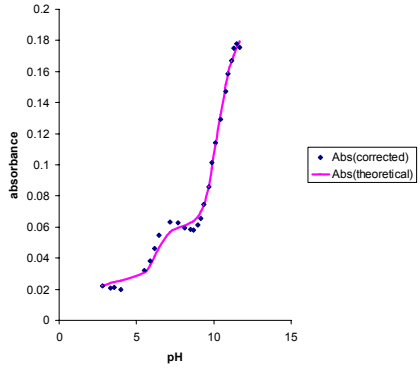

d.)

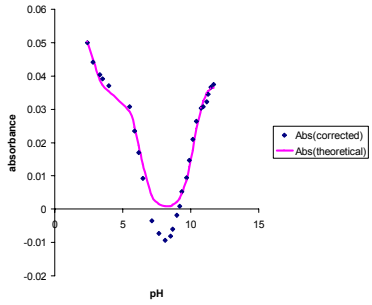

Figure 21: Comparison of corrected absorbance versus theoretical absorbance with respect to pH at wavelengths of a.) 241 nm, b.) 259 nm, c.) 287 nm, and d.) 313 nm for the titration of PDOX with Pb(II).

a.)

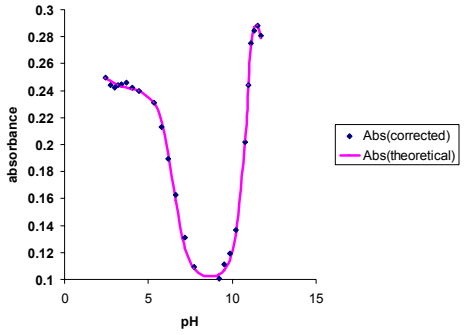

b.)

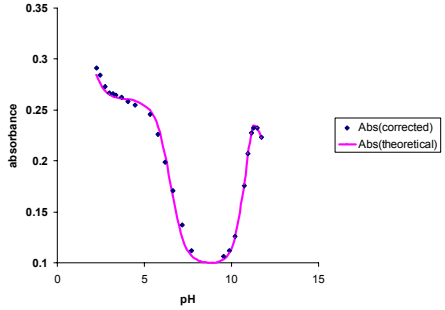

c.)

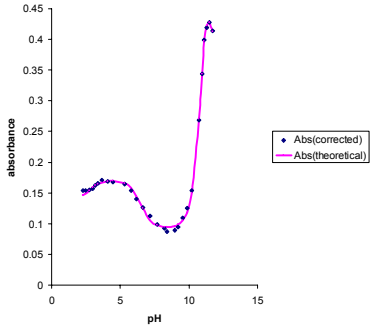

d.)

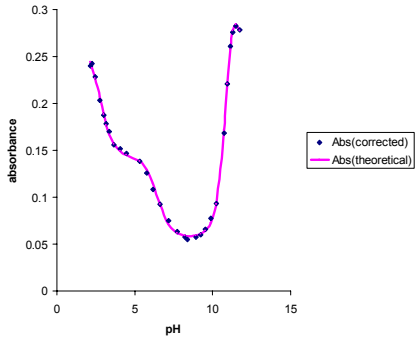

Figure 22: Comparison of corrected absorbance versus theoretical absorbance with respect to pH at wavelengths of a.) 241 nm, b.) 259 nm, c.) 287 nm and d.) 313 nm for the titration of PDOX with Zn (II).

complex was calculated to be 9.71. A $\Delta \log K_1$ of 2.48 shows a significant difference in stability between the PDOX complex and the 1, 10-phenathroline complex of Zn (II).

Fluorescence of PDOX and metal-PDOX complexes

EEM (excitation and emission) fluorescence spectra for both the free ligand and metal-ligand complexes were obtained using a Jobin Yvon SPEX Fluoromax-3 scanning fluorometer equipped with a 150 W Xe arc lamp and a R928P detector. Excitation wavelengths were scanned from 250 to 500 nm at 4 nm intervals and emission wavelength were scanned from 280 nm to 550 nm at 4 nm intervals. The intensity of fluorescence was monitored at an excitation wavelength of 275 nm and an emissions wavelength of 415 nm. The increase in intensity of the metal-PDOX complex was compared to that of the free PDOX intensity at these wavelengths. An EEM (excitation and emission) spectra of DI water used in each sample was taken to prevent mistaking that fluorescence for the fluorescence of the ligand. The free PDOX spectrum and DI water spectrum can be seen in Figure 23.

PDOX undergoes chelation enhanced fluorescence known as the CHEF Effect.[2] PDOX has a highly aromatic backbone, which gives it the capability of fluorescing intensely. However, the lone pair of electrons on each nitrogen atom within the aromatic backbone quench the fluorescence. Therefore, an increase of fluorescence is seen as the nitrogen atoms of PDOX complex with a metal ion, and are no longer available to quench the fluorescence. Metal ions with the ideal ionic radius (1.20 Å) to form a complex with PDOX should posses the highest increase in fluorescence. Table 3 shows the increase in fluorescence of the metal-ligand complex compared to the free ligand.

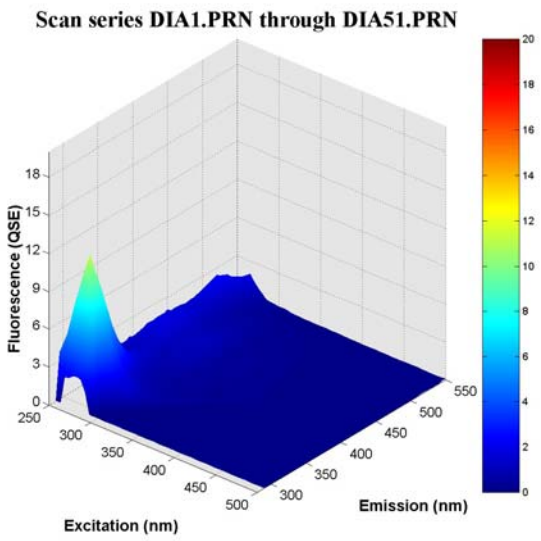

a.)

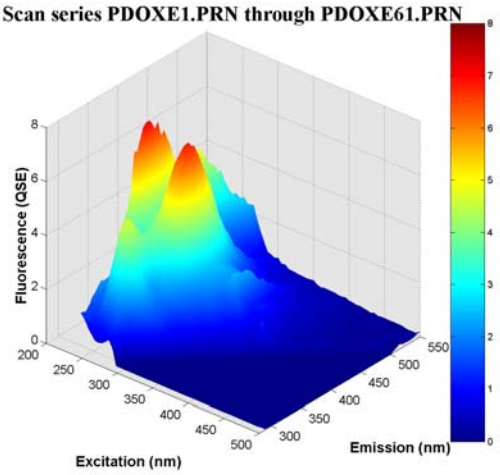

b.)

Figure 23: EEM (excitation and emission) three dimensional spectra for a.) DI water and b.) free PDOX.

Table 3: Fluorescence intensity of free PDOX compared to the intensity of fluorescence of the metal-PDOX complex.

	Intensity	Δ Intensity
PDOX	**4.41**	
Ca(II)	**7.22**	**2.81**
Cd(II)	**9.31**	**4.90**
Pb(II)	**18.19**	**13.78**
Hg(II)	**5.11**	**0.70**
Zn(II)	**4.55**	**0.14**

Free PDOX results

A $1x10^{-6}$ M PDOX solution was made and the intensity of fluorescence was recorded at an excitation wavelength of 275 nm and an emission wavelength of 415 nm. The intensity of free PDOX was 4.41. This value was used to determine the increase in fluorescence of various metal-PDOX complexes compared to free PDOX. Figure 23(b) shows the EEM spectra of free PDOX.

PDOX-calcium (II) results

A 1:1 PDOX to calcium solution was prepared and the intensity of fluorescence was measured at an excitation wavelength of 275 nm and an emission wavelength of 415 nm. The EEM spectra can be seen in Figure 24. The intensity of the calcium-PDOX complex was recorded to be 7.22. This shows a 64 % increase in fluorescence compared to that of the free ligand. Calcium (II) has an ionic radius of 0.99 Å. Figure 25 shows a HyperChem generated calcium-PDOX complex. This figure shows that calcium has an ionic radius which is close to the ideal metal ion radius for forming a complex with PDOX, leading to increased fluorescence.

PDOX-cadmium (II) results

A 1:1 PDOX to cadmium solution was prepared and the intensity of fluorescence was measured at an excitation wavelength of 275 nm and an emission wavelength of 415 nm. The EEM spectra can be seen in Figure 26. The intensity of the cadmium-PDOX complex was recorded to be 9.31. This shows a 111 % increase in fluorescence compared to that of the free ligand. Cadmium (II) has an ionic radius of 0.97 Å. Figure

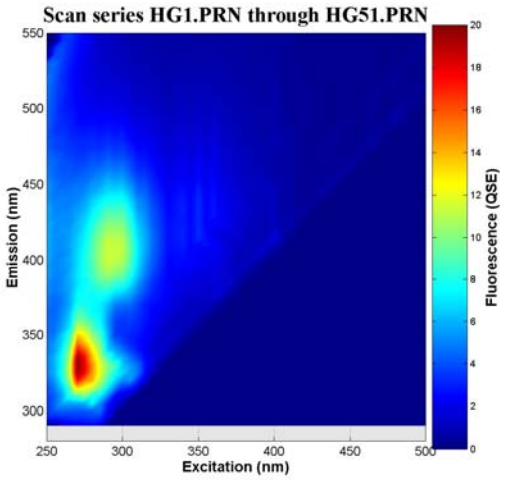

a.)

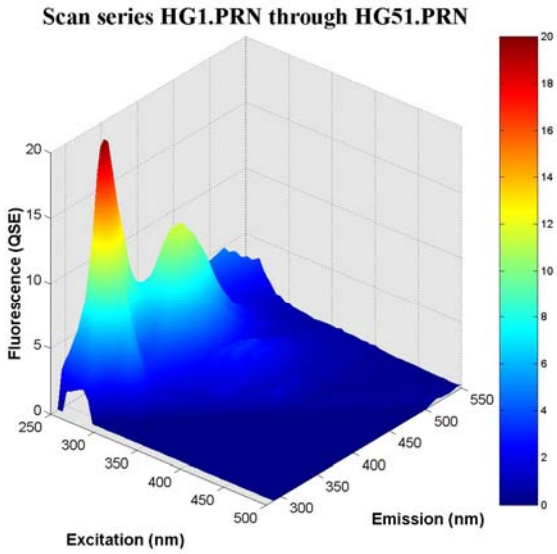

b.)

Figure 24: EEM spectra for the calcium-PDOX complex both a.) two dimensional and b.) three dimensional.

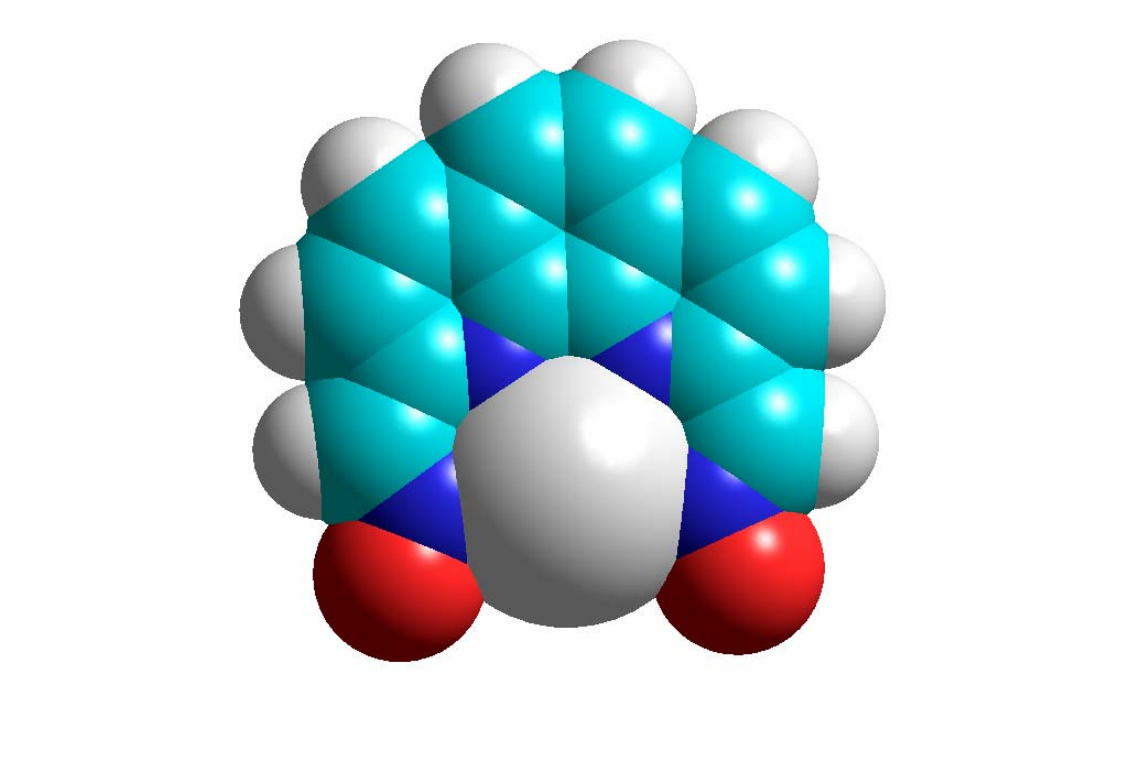

Figure 25: HyperChem generated calcium-PDOX complex using the MM+ force field.

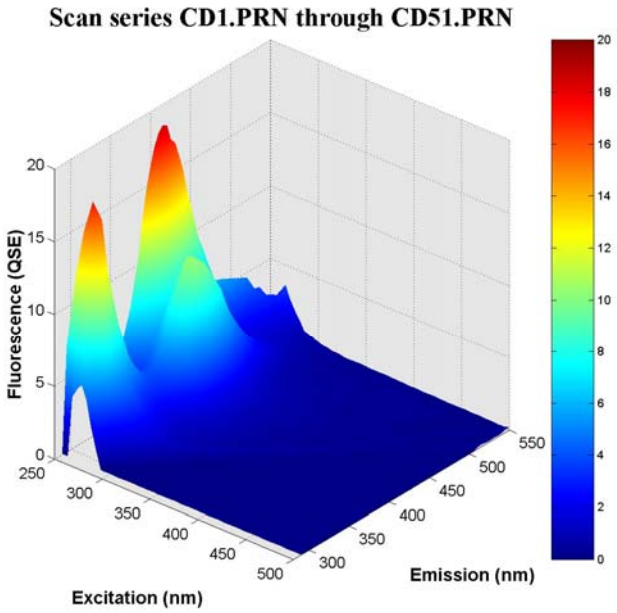

a.)

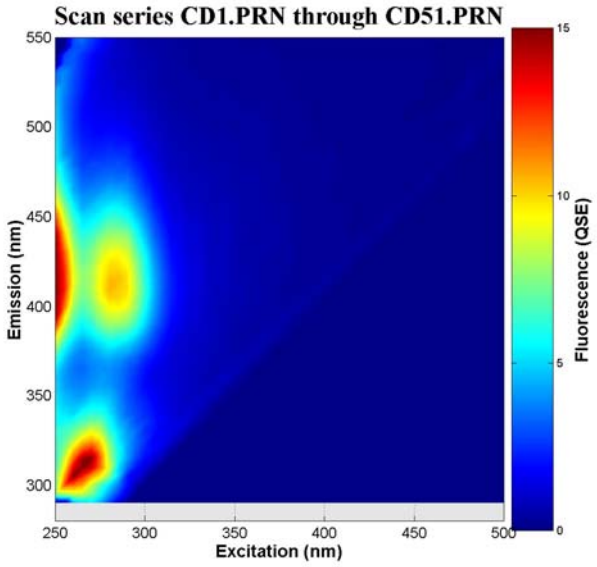

b.)

Figure 26: EEM spectra for the cadmium-PDOX complex both a.) three dimensional and b.) two dimensional.

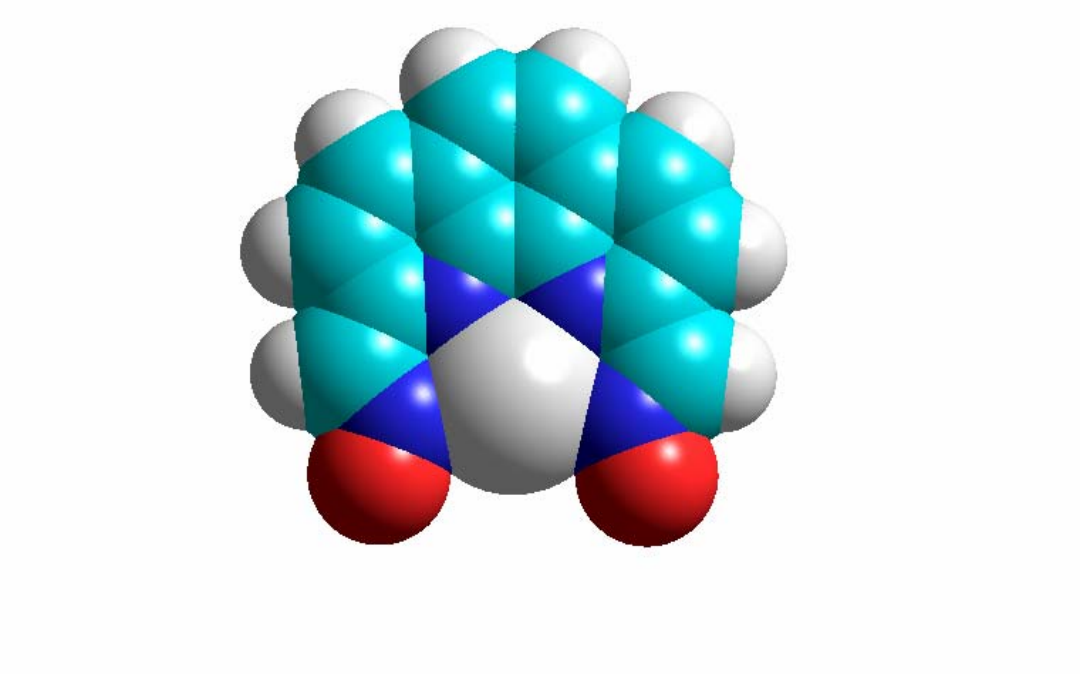

Figure 27: HyperChem generated cadmium-PDOX complex using the MM+ force field.

27 shows a HyperChem generated cadmium-PDOX complex. This figure shows that cadmium like calcium has an ionic radius which is close to the ideal metal ion radius for forming a complex with PDOX, leading to increased fluorescence.

PDOX-lead (II) results

A 1:1 PDOX to lead solution was prepared and the intensity of fluorescence was measured at an excitation wavelength of 275 nm and an emission wavelength of 415 nm. The EEM spectra can be seen in Figure 28. The intensity of the lead-PDOX complex was recorded to be 18.19. This shows a substantial 312 % increase in fluorescence compared to that of the free ligand. Lead (II) has an ionic radius of 1.19 Å. Figure 29 shows the crystal structure of the lead-PDOX complex. This figure shows that lead (II) has an ideal ionic radius for forming a complex with PDOX, leading to a dramatic increase in fluorescence.

PDOX-mercury (II) results

A 1:1 PDOX to mercury solution was prepared and the intensity of fluorescence was measured at an excitation wavelength of 275 nm and an emission wavelength of 415 nm. The EEM spectra can be seen in Figure 30. The intensity of the mercury-PDOX complex was recorded to be 5.11. This shows a slight 16 % increase in fluorescence compared to that of the free ligand. Mercury (II) has an ionic radius of 1.02 Å. Figure 31 shows a HyperChem generated mercury-PDOX complex. This figure shows that mercury has an ionic radius which is close to the ideal metal ion radius for

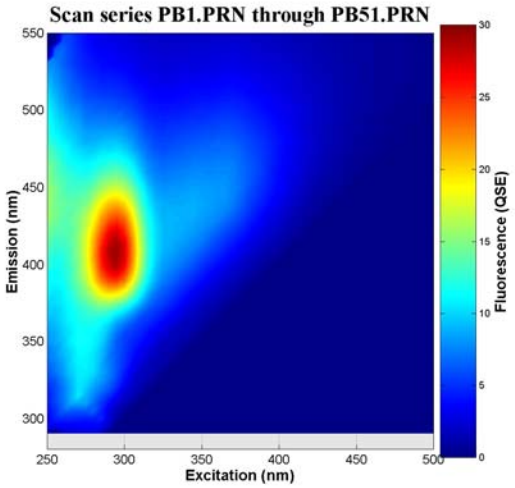

a.)

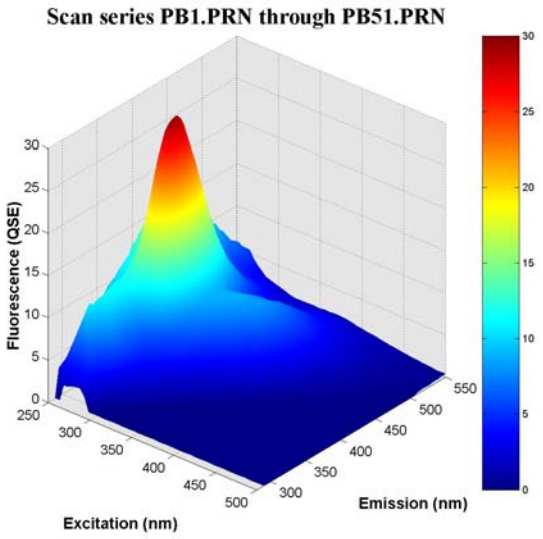

b.)

Figure 28: EEM spectra for the lead-PDOX complex both a.) two dimensional and b.) three dimensional.

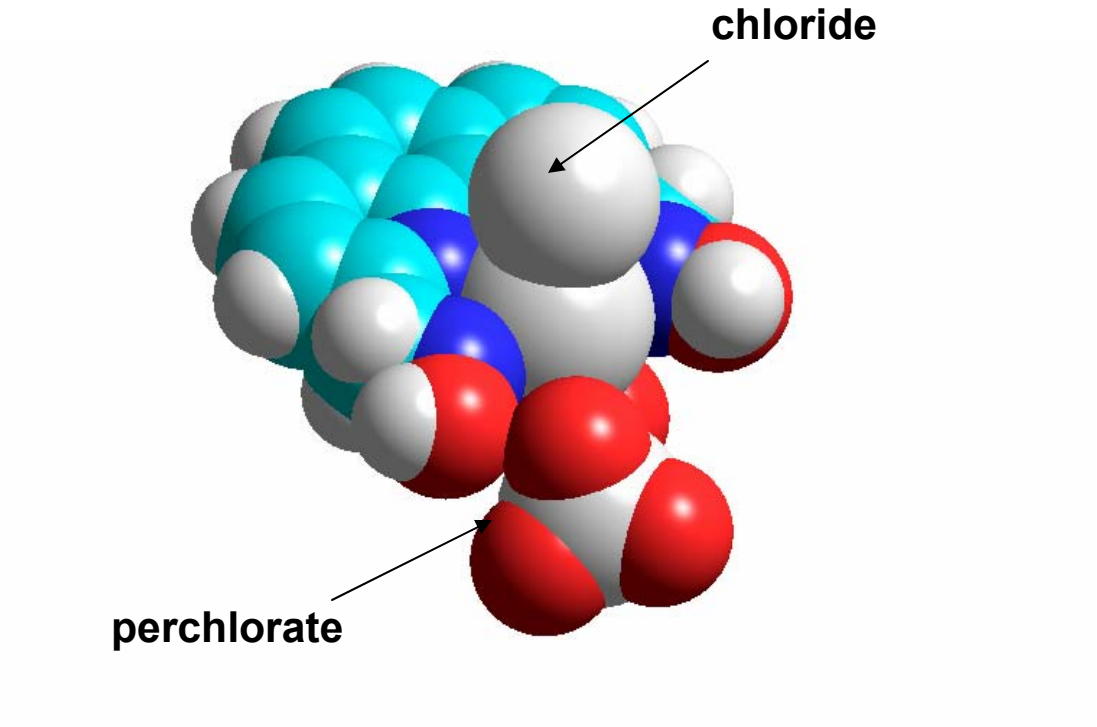

Figure 29: Crystal structure of the lead-PDOX complex, see appendix for details.

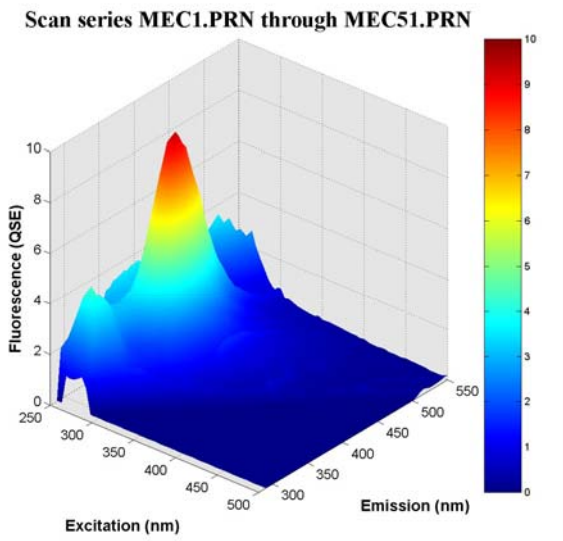

a.)

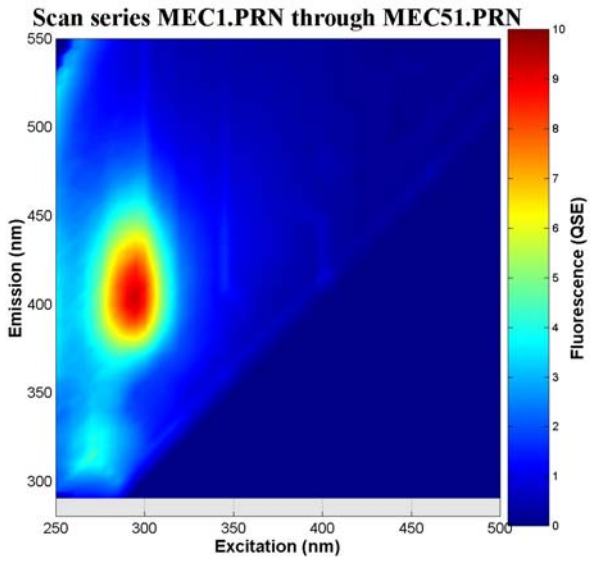

b.)

Figure 30: EEM spectra for the mercury-PDOX complex both a.) three dimensional and b.) two dimensional.

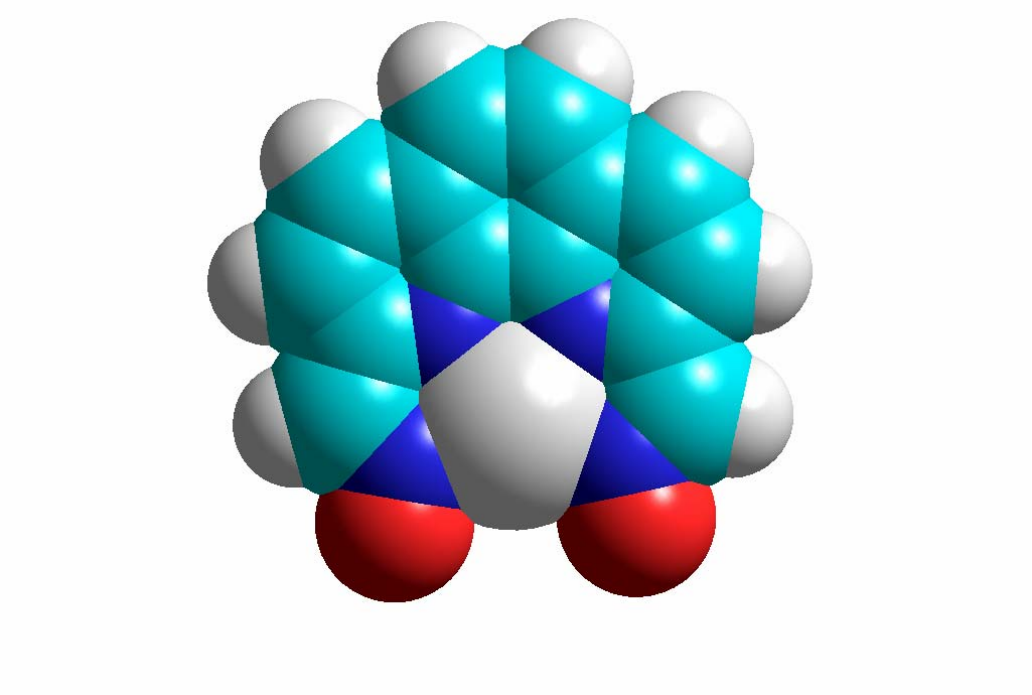

Figure 31: HyperChem generated mercury-PDOX complex using the MM+ force field. Axial waters omitted for clarity.

forming a complex with PDOX, leading to slight increase in fluorescence. Mercury is categorized as a soft metal ion preferring soft donor atoms such as iodine.[31] A particular problem with Hg is its preference for linear coordination geometry. It may thus be that the N-donors on the 1,10-phenanthroline part of PDOX are not coordinated to the Hg(II), and thus act to quench fluorescence.[32] This might explain why there is not a substantial increase in fluorescence even though the ionic radius is similar in size to previously discussed metal ions (Cd(II) and Ca(II)).

PDOX-zinc (II) results

A 1:1 PDOX to zinc solution was prepared and the intensity of fluorescence was measured at an excitation wavelength of 275 nm and an emission wavelength of 415 nm. The EEM spectra can be seen in Figure 32. The intensity of the zinc-PDOX complex was recorded to be 4.55. This shows a negligible 3 % increase in fluorescence compared to that of the free ligand. Zinc (II) has an ionic radius of 0.74 Å. Figure 33 shows a HyperChem generated zinc-PDOX complex. This figure shows that zinc has a smaller ionic radius than the ideal radii needed for complexing with PDOX.

UV-Vis spectrophotometric titrations Involving DIPHEN

UV/Vis spectroscopy was used as an analytical tool to determine the stability constants ($\log K_1$) of the metal-DIPHEN complexes. For each titrant addition of 0.1 *M* NaOH absorbance scans were taken from 190 nm to 350 nm. Absorbance data were taken at selected wavelengths of 227,259, 279, 296 ,and 312 nm. Peak shifts were seen for these wavelengths upon complexation of DIPHEN with a metal ion.

In order to determine the protonation constants for the ligand, DIPHEN, titrations were performed at 25.0± 0.1 ˚C at 0.1 *M* ionic strength (0.1 *M* $NaClO_4$). Figure 34 shows absorbance versus wavelength (nm) scans at pH values of approximately 2.00 to 7.00 as an overlay. Absorbance data from selected wavelengths was used to generate plots of absorbance versus pH. This data was then used to calculate the protonation constants for DIPHEN. DIPHEN as a free ligand has two separate protonation events pK_1, and pK_2. These protonation events can be seen in Figure 35.

UV-Vis spectrophotometric titrations involving metals with DIPHEN

For metal-DIPHEN titrations absorbance data were generated from 227,259, 279, 296, and 312 nm. Data was taken from wavelengths experiencing the most shifting upon complexation. The formation constants for each metal ion with DIPHEN were determined using equations 1-16. The exception being that DIPHEN has only two protonation constants. Apparent protonation constants of the metal-DIPHEN complex were determined using plots of corrected absorbance and theoretical absorbance versus pH. Then the difference of the pK_a values relative to the free ligand were taken and negative log of the concentration of the free metal was added to this values, thus giving the logK_1 of the metal-DIPHEN complex.

Molecular mechanics calculations were performed for metal ions with DIPHEN and a plot of energy (kcal/mol) versus metal-nitrogen bond length (Å) was generated, which is illustrated in Figure 36. A minimum nitrogen to metal bond length was

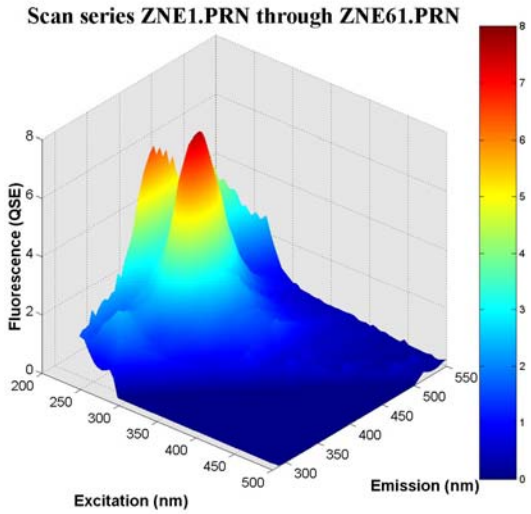

a.)

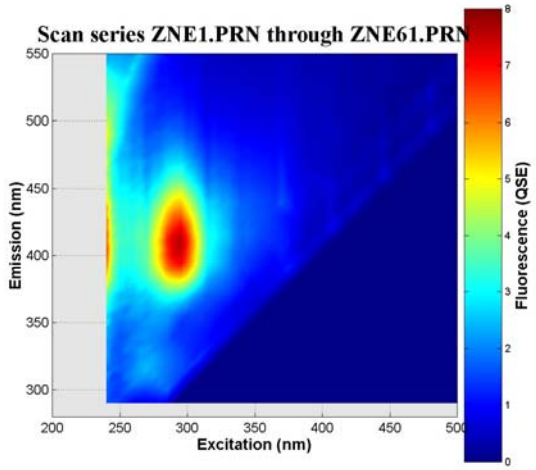

b.)

Figure 32: EEM spectra for the zinc-PDOX complex both a.) three dimensional and b.) two dimensional.

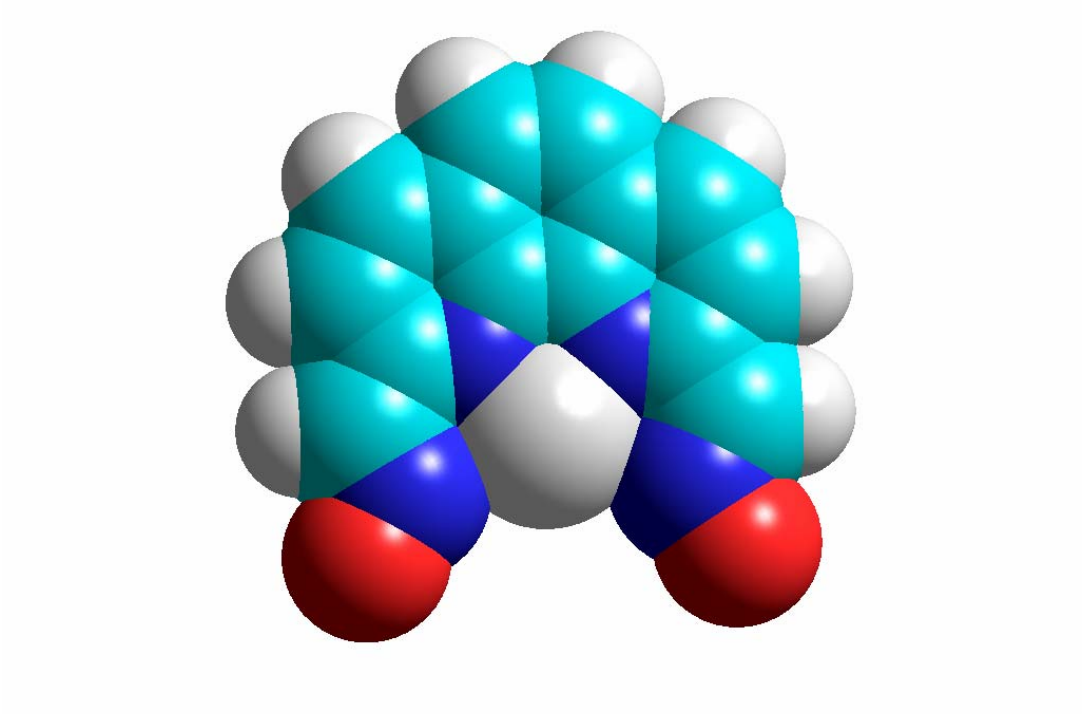

Figure 33: HyperChem generated zinc-PDOX complex using the MM+ force field. Axial waters omitted for clarity.

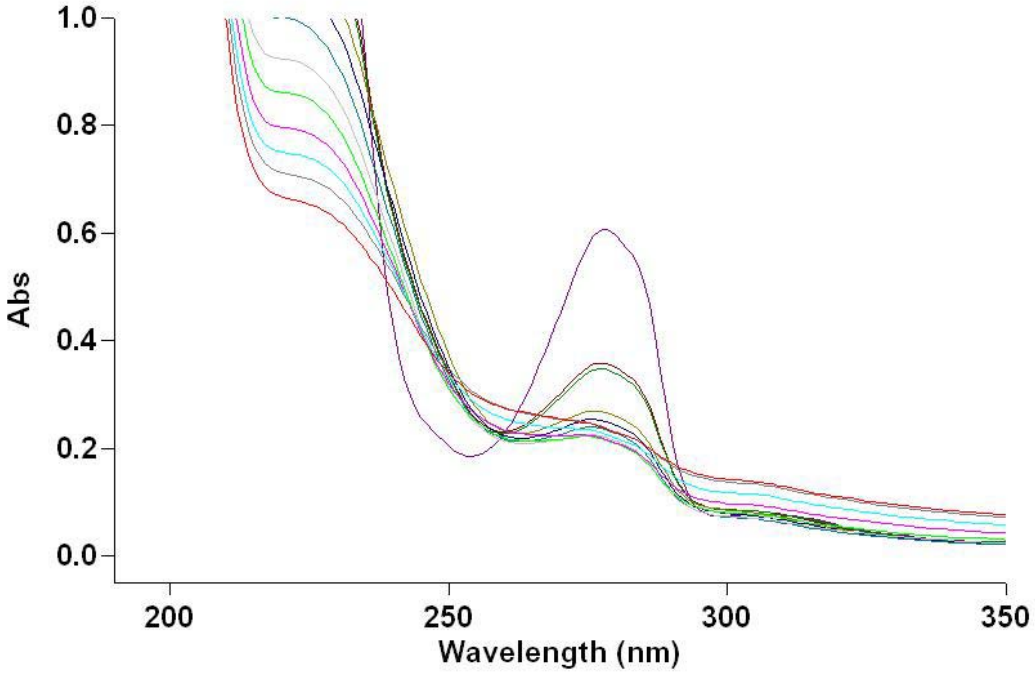

Figure 34: UV absorbance spectra for the titration of DIPHEN ($1x10^{-6}$ *M*) at 25.0±0.1 ˚C, at 0.1 *M* ionic strength, and at a pH range of approximately 2.00 to 7.00.

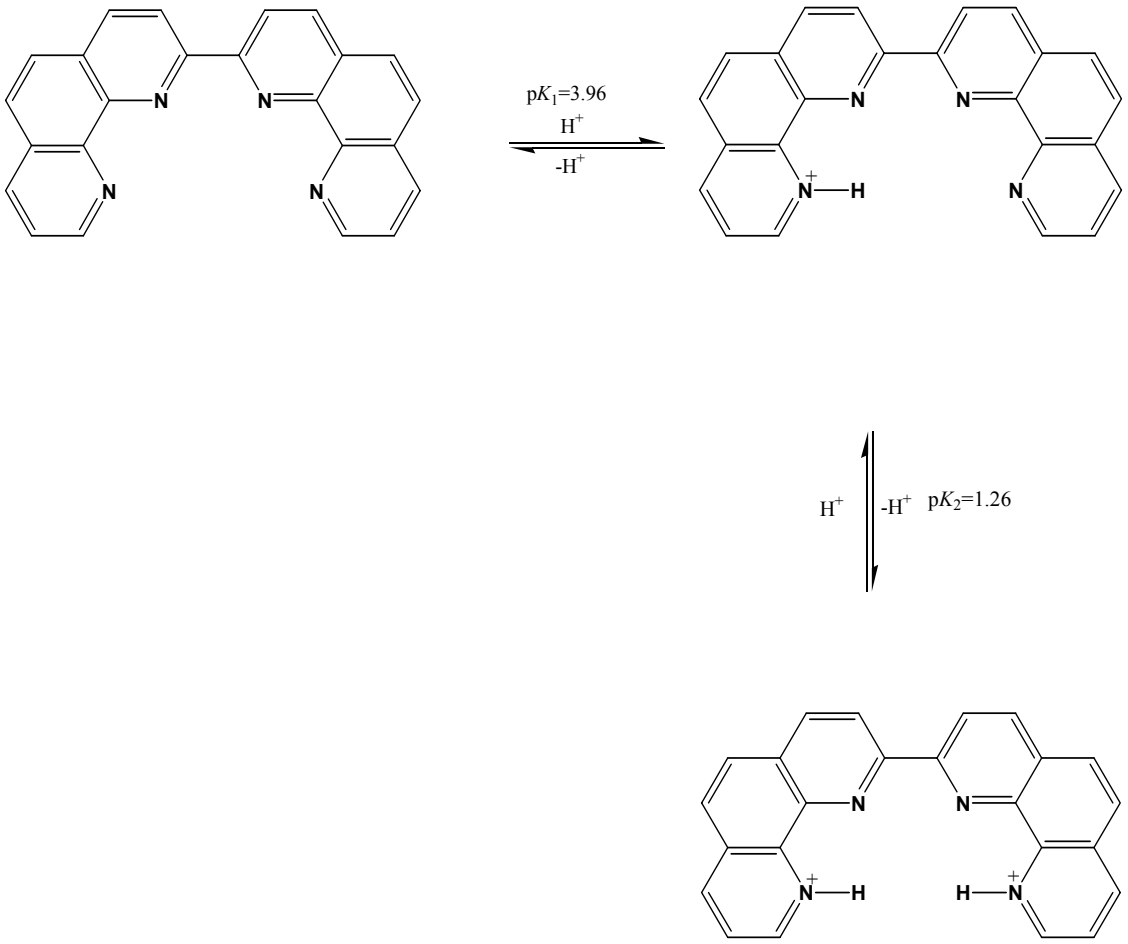

Figure 35: The two protonation events of DIPHEN.

observed to be 2.29 Å. This calculation allows for an estimation of an ideal metal ion ionic radius, the result being approximately 1.00 Å. This corresponds with metals such as Ca(II) and Cd(II). The stability constants, log K_1, for metals with DIPHEN calculated from titration experiment complemented the results from the MM calculations. Slight variations were observed which were due to metal ion selectivity for nitrogen donor atoms.

The stability constants determined with metal ions with DIPHEN from UV-Vis spectroscopy titration experiments can be seen in Table 4. The stability constants are compared to that of 1,10-phenanthroline which is also displayed in Table 4. Several metal-DIPHEN complexes showed an increase in stability due to the addition of the second phenanthroline ring which contains two additional nitrogen donors. However, two smaller metal ions did show a decrease in logK_1 value for DIPHEN compared to 1,10-phenanthroline due to their smaller ionic radii.

DIPHEN-calcium(II) results

Calcium(II) has an ionic radius of 0.99 Å, which is ideal for complexing with DIPHEN. The UV absorbance spectra are shown in Figure 37 for the titration of Ca(II) with PDOX. The corrected absorbance and theoretical absorbance versus pH plots are shown in Figure 38. From the selected wavelengths previously described, apparent pK_a values were seen at 3.55 and 1.39. Using equations 1-16, a logK_1 value for the calcium-DIPHEN complex was calculated to be 1.74. A Δ logK_1 of 0.74 shows a quantitative

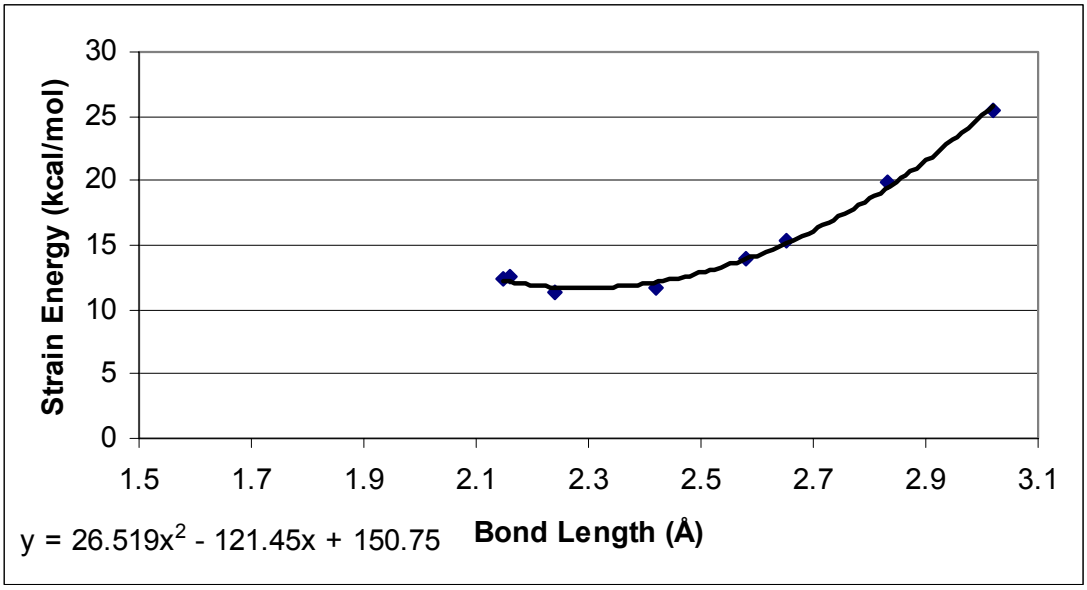

Figure 36: Calculated strain energy (kcal/mol) versus metal nitrogen bond length (Å) for metal-DIPHEN complexes.

Table 4: Comparison of log K_1 data for metal ions with DIPHEN and 1,10-phenanthroline.

Metal	Ionic Radius (Å)	log K_1DIPHEN (ML)	log K_1 with 1,10-phen(ML)	Δ log $K1$
Ca(II)	0.99	1.74	1	0.74
Cd(II)	0.97	5.88	5.4	0.48
Cu(II)	0.57	7.37	9.7	-2.33
Gd(III)	0.938	6.35		
La(III)	1.061		2.1	
Pb(II)	1.19	6.94	4.6	2.34
Zn(II)	0.74	5.98	6.4	-0.42

difference in stability between the PDOX complex and the 1,10-phenathroline complex of Ca(II).

DIPHEN-cadmium(II) results

The ionic radius of cadmium(II) is 0.95 Å, which again is close to the ideal metal ion size for forming a stable complex with DIPHEN. The UV absorbance spectra are shown in Figure 39 for the titration of Cd(II) with DIPHEN. Also, the corrected absorbance and theoretical absorbance versus pH plots are shown in Figure 40. From the selected wavelengths previously described, apparent pK_a values were seen at 4.21 and 2.93. Using equations 1-16, a logK_1 values for the cadmium-DIPHEN complex was calculated to be 5.88. A Δ logK_1 of 0.48 shows a quantitative difference in stability between the DIPHEN complex and the 1,10-phenathroline complex of Cd(II).

PDOX-copper(II) results

Copper(II) has an ionic radius of 0.57 Å, which is smaller than the desired ionic radius for complexing with DIPHEN. The UV absorbance spectra are shown in Figure 41 for the titration of Cu(II) with DIPHEN. Also, the corrected absorbance and theoretical absorbance

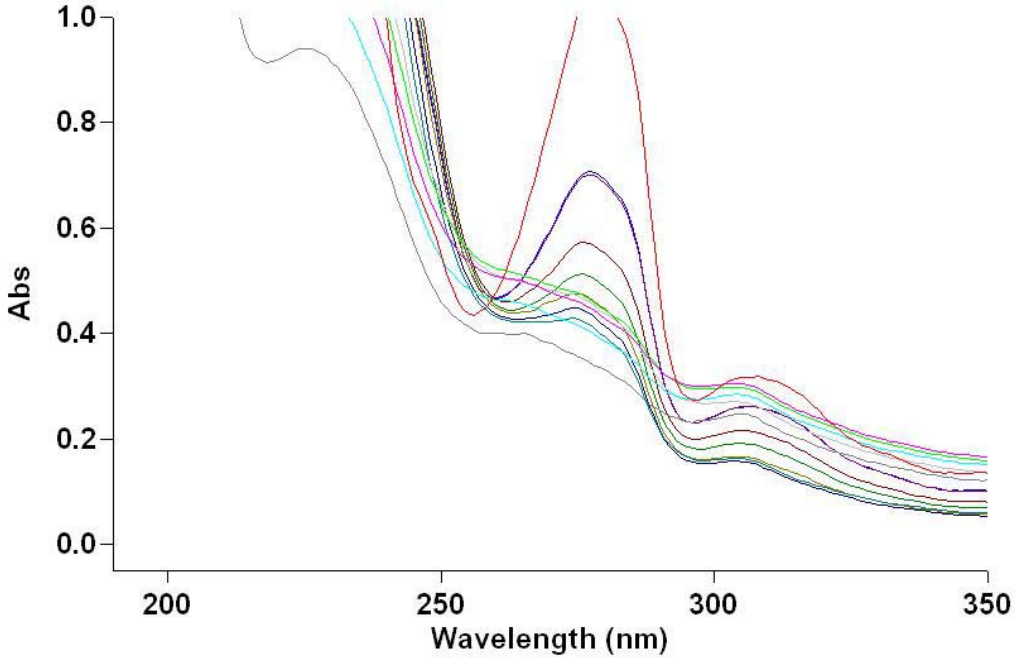

Figure 37: UV absorbance spectra for the titration of Ca(II) (0.0333 *M*) and DIPHEN ($1x10^{-6}$ *M*) at 25.0±0.1 ˚C, at 0.1 *M* ionic strength, and at a pH range of approximately 2.00 to 7.00.

a.)

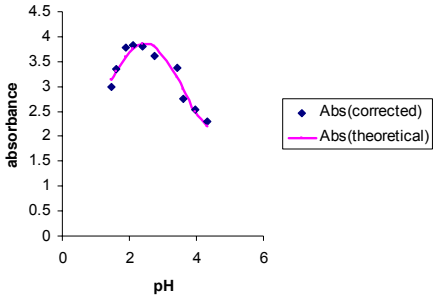

b.)

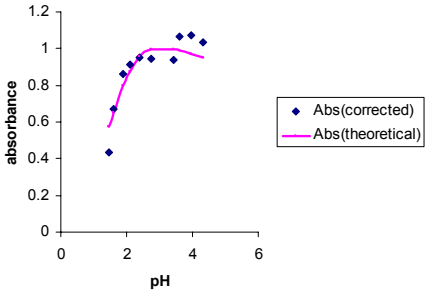

c.

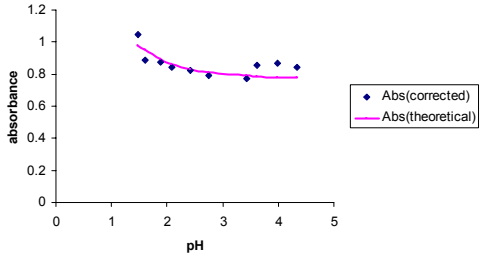

d.

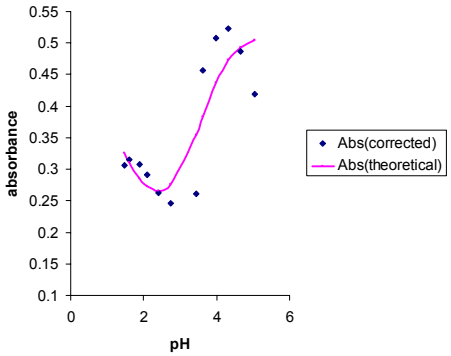

Figure 38: Comparison of corrected absorbance versus theoretical absorbance with respect to pH at wavelengths of a.) 259 nm, b.) 279 nm, c.) 296 nm and d.) 312 nm for the titration of DIPHEN with Ca (II).

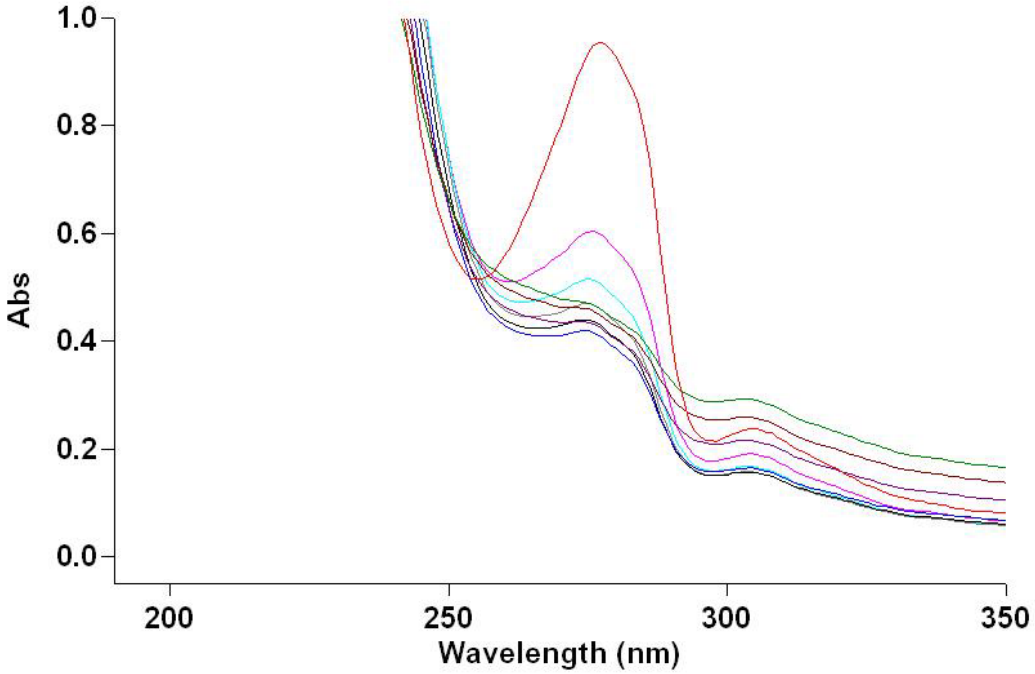

Figure 39: UV absorbance spectra for the titration of Cd(II) ($1x10^{-6}$ *M*) and DIPHEN ($1x10^{-6}$ M) at 25.0±0.1 ˚C, at 0.1 *M* ionic strength, and at a pH range of approximately 2.00 to 7.00.

a.)

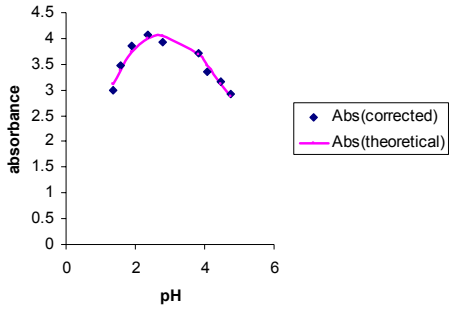

b.)

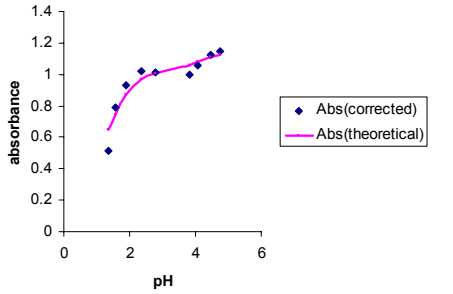

c.)

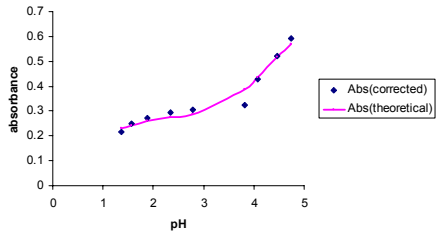

d.)

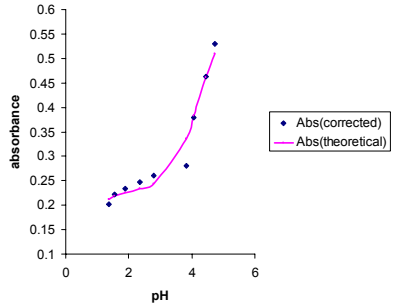

Figure 40: Comparison of corrected absorbance versus theoretical absorbance with respect to pH at wavelengths of a.) 227 nm, b.) 255 nm, c.) 296 nm and d.) 312 nm for the titration of DIPHEN with Cd (II).

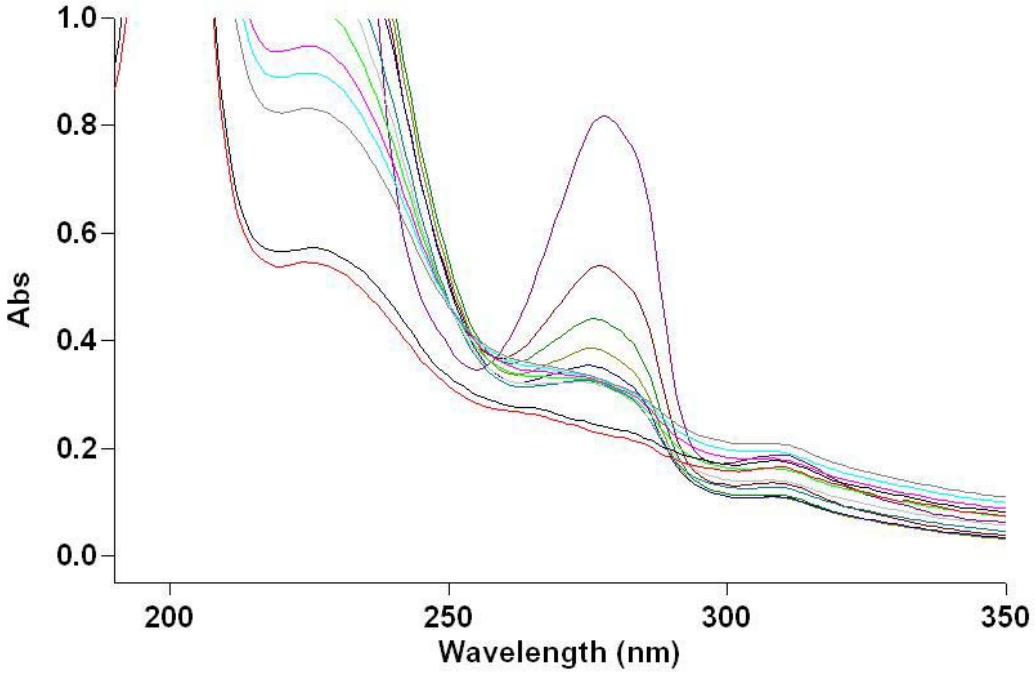

Figure 41: UV absorbance spectra for the titration of Cu(II) ($1x10^{-6}$ *M*) and DIPHEN ($1x10^{-6}$ *M*) at 25.0±0.1 ˚C, at 0.1 *M* ionic strength, and at a pH range of approximately 2.00 to 7.00.

versus pH plots are shown in Figure 42. From the selected wavelengths previously described, apparent pK_a values were seen at 2.61 and 1.54. Using equations 1-16, a logK_1 value for the copper-DIPHEN complex was calculated to be 7.37. A Δ logK_1 of -2.33 shows a quantitative difference in stability between the DIPHEN complex and the 1,10-phenathroline complex of Cu(II).

DIPHEN-gadolinium(III) results

Gadolinium(III) has an ionic radius of 0.93 Å, which is almost ideal for complexing with DIPHEN. The UV absorbance spectra are shown in Figure 43 for the titration of Gd(III) with DIPHEN. Also, the corrected absorbance and theoretical absorbance versus pH plots are shown in Figure 44. From the selected wavelengths previously described, apparent pK_a values were seen at 3.67 and 1.20. Using equations 1-16, a logK_1 value for the gadolinium-DIPHEN complex was calculated to be 6.35. There was no logK_1 reported for 1,10-phenanthroline with Gd(III) to compare DIPHEN with. In order to approximate the Δ logK_1 a comparison of known logK_1 values with lanthanum(III) can be used due to its similar chemistry with gadolinium(III).[32] This would give an approximate Δ logK_1 of 4.20 when compared to that of 1,10-phenanthroline.

DIPHEN-lead(II) results

Lead(II) has an ionic radius of 1.19 Å, which is slightly larger than the desired ionic radius for complexing with DIPHEN. The UV absorbance spectra are shown in Figure 45 for the titration of Pb(II) with DIPHEN. The corrected absorbance and

a.)

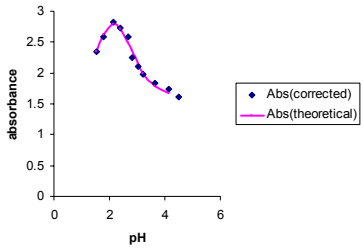

b.)

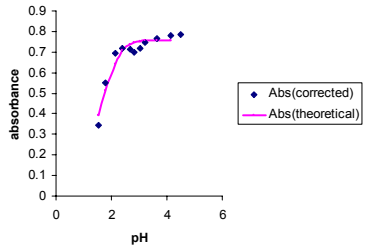

c.)

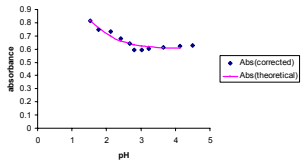

d.)

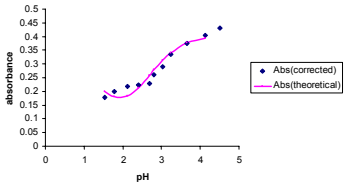

e.)

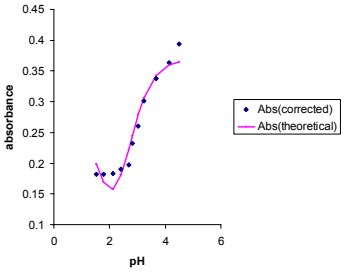

Figure 42: Comparison of corrected absorbance versus theoretical absorbance with respect to pH at wavelengths of a.) 227 nm, b.) 255 nm, c.) 279 nm, d.) 296 nm and e.) 312 nm for the titration of DIPHEN with Cu (II).

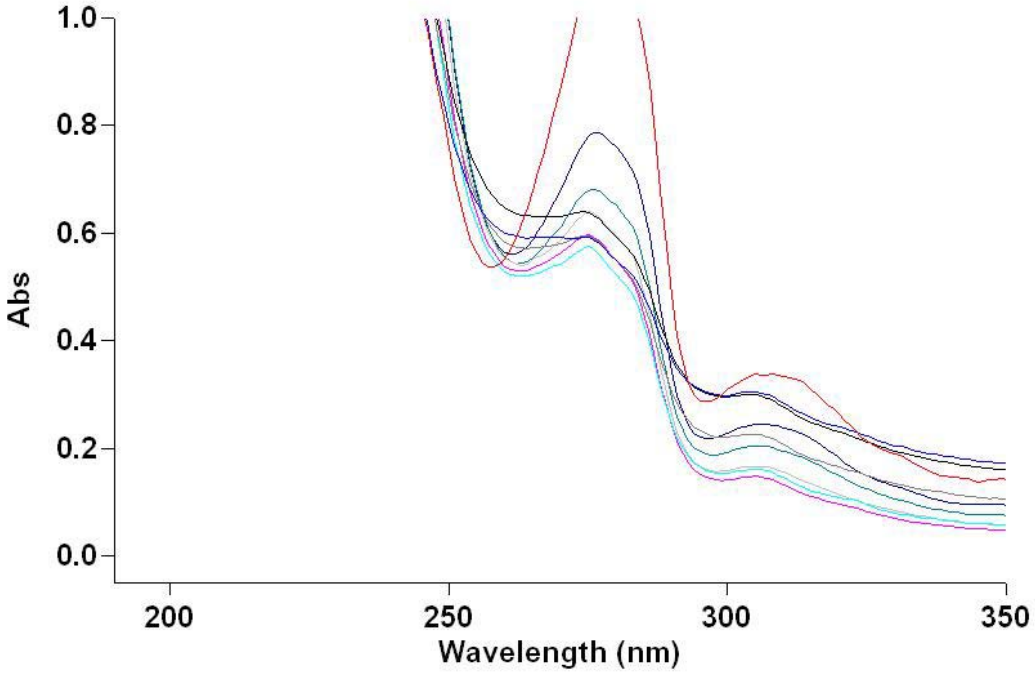

Figure 43: UV absorbance spectra for the titration of Gd(III) ($1x10^{-6}$ *M*) and DIPHEN ($1x10^{-6}$ *M*) at 25.0±0.1 ˚C, at 0.1 *M* ionic strength, and at a pH range of approximately 2.00 to 7.00.

a.)

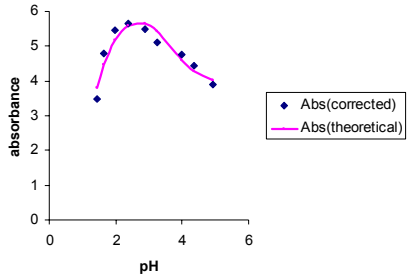

b.)

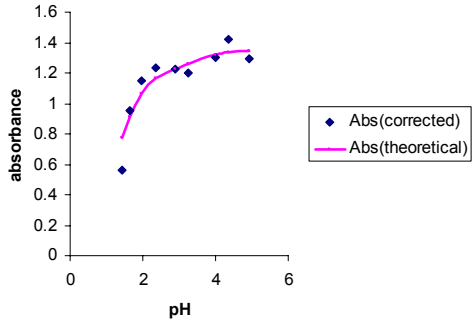

c.)

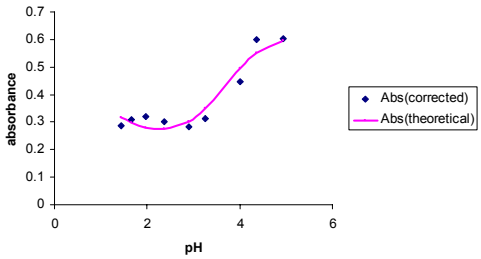

d.)

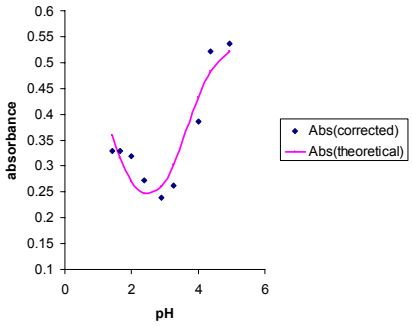

Figure 44: Comparison of corrected absorbance versus theoretical absorbance with respect to pH at wavelengths of a.) 227 nm, b.) 255 nm, c.) 296 nm and d.) 312 nm for the titration of DIPHEN with Gd(III).

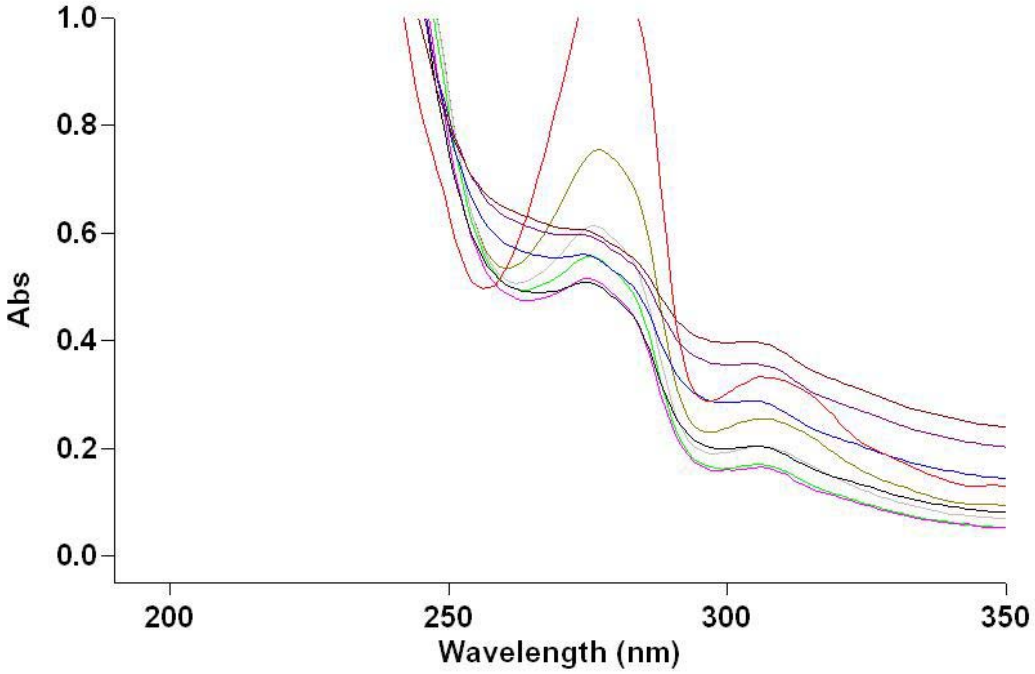

Figure 45: UV absorbance spectra for the titration of Pb(II) ($1x10^{-6}$ *M*) and DIPHEN ($1x10^{-6}$ *M*) at 25.0±0.1 ˚C, at 0.1 *M* ionic strength, and at a pH range of approximately 2.00 to 7.00.

a.)

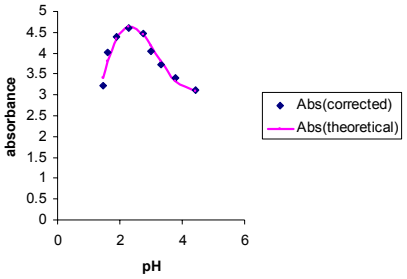

b.)

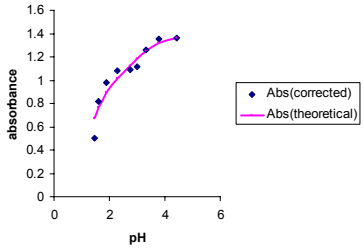

c.)

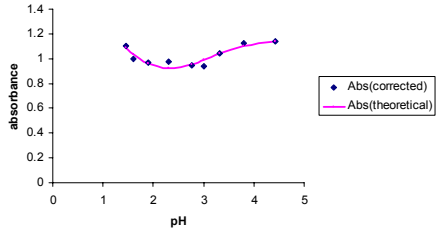

d.)

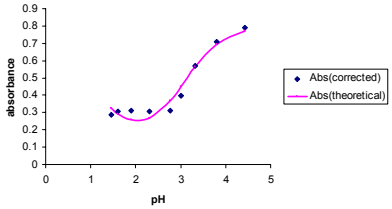

e.)

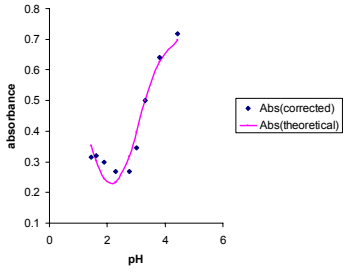

Figure 46: Comparison of corrected absorbance versus theoretical absorbance with respect to pH at wavelengths of a.) 227 nm, b.) 255 nm, c.) 279 nm, d.) 296 nm and e.) 312 nm for the titration of DIPHEN with Pb (II).

theoretical absorbance versus pH plots are shown in Figure 46. From the selected wavelengths previously described, apparent pK_a values were seen at 3.07 and 1.19. Using equations 1-16, a logK_1 value for the lead-DIPHEN complex was calculated to be 6.94. A Δ logK_1 of 2.34 shows a quantitative difference in stability between the DIPHEN complex and the 1,10-phenathroline complex of Pb(II).

DIPHEN-zinc(II) results

Zinc (II) has an ionic radius of 0.74 Å, which is smaller than the ideal ionic radius for complexing with DIPHEN. The UV absorbance spectra are shown in Figure 47 for the titration of Zn(II) with DIPHEN. The corrected absorbance and theoretical absorbance versus pH plots are shown in Figure 48. From the selected wavelengths previously described, apparent pK_a values were seen at 3.96 and 1.26. Using equations 1-16, a logK_1 value for the zinc-DIPHEN complex was calculated to be 5.98. A Δ logK_1 of -0.42 shows a quantitative difference in stability between the DIPHEN complex and the 1,10-phenathroline complex of Zn(II).

CONCLUSION

In the past both macrocycles and cryptands have shown an increase in metal-ligand complex stability due to their high levels of preorganization. The latter type of preorganization derives from cyclization to give the ring structures of these ligands. The restricted number of conformations available to the free ligand, as compared to non-cyclic analogues, leads to higher complex stability. However, it has been shown that macrocycles still have a large number of conformations available to them that can

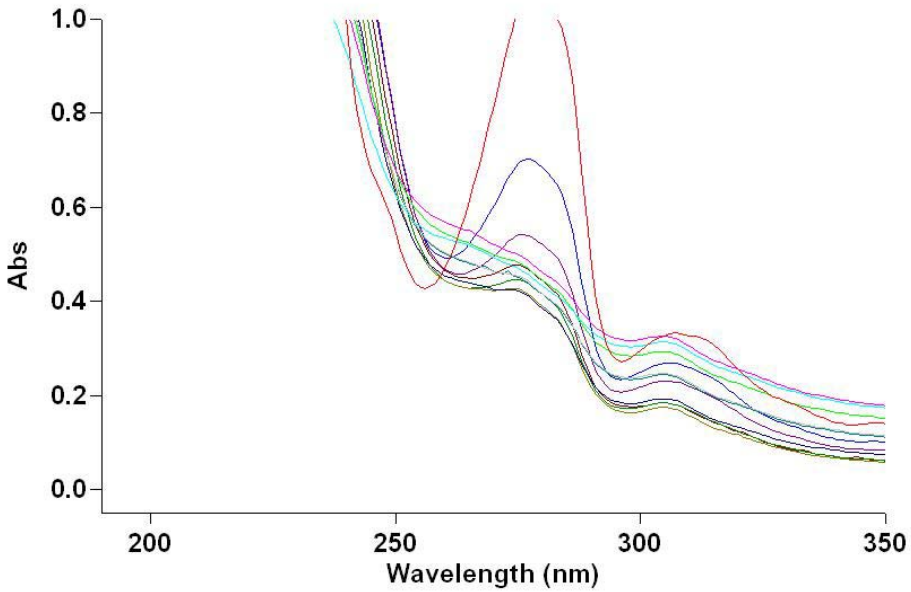

Figure 47: UV absorbance spectra for the titration of Zn(II) ($1x10^{-6}$ *M*) and DIPHEN ($1x10^{-6}$ *M*) at 25.0±0.1 ˚C, at 0.1 *M* ionic strength, and at a pH range of approximately 2.00 to 7.00.

a.)

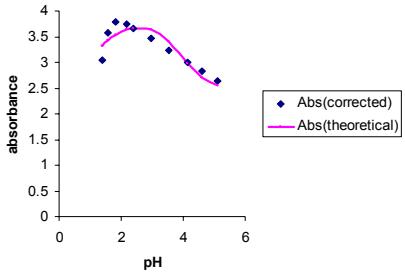

b.)

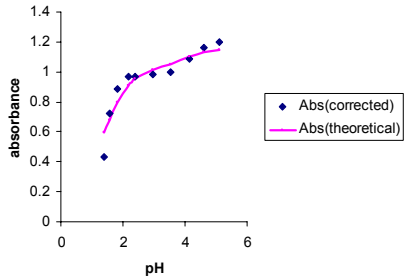

c.)

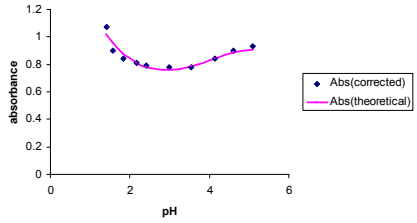

d.)

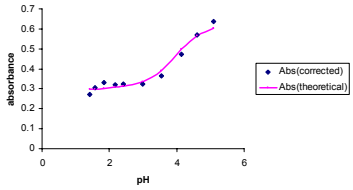

e.)

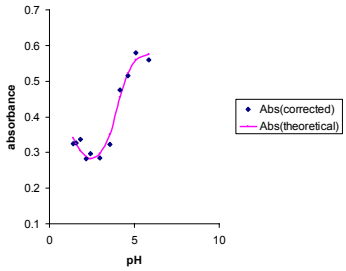

Figure 48: Comparison of corrected absorbance versus theoretical absorbance with respect to pH at wavelengths of a.) 227 nm, b.) 255 nm, c.) 279 nm, d.) 296 nm and e.) 312 nm for the titration of DIPHEN with Zn (II).

accommodate metal ions of different sizes, so that the increase in metal ions size-based selectivity is not observed. The rigid aromatic backbones of the ligands PDOX and DIPHEN studied here should lead to a greatly increased metal ion size-based selectivity, which is observed. Both PDOX and DIPHEN are rigid molecules which form more stable complexes with metal ions that match the size selectivity of the ligands. 1, 10-phenanthroline-2, 9-dialdoxime (PDOX) shows selectivity for larger metal ions with an ionic radius of approximately 1.20Å. Bis-1, 10-phenanthroline (DIPHEN) shows selectivity for larger metal ions with an ionic radius of approximately 1.00Å. Both ligands form five membered chelate rings which favor larger metal ions. Both ligands contain four nitrogen donor atoms, but form complexes of considerably greater thermodynamic stability than other tetradentate ligands. The fluorescence properties of the PDOX complexes suggest that ligands of this type should be useful in the design of fluorescence sensors for large metal ions such as Cd(II), Pb(II), and Ca(II), which should be of both biological and medicinal interest. Nitrogen donor atoms are classified as intermediate bases on Pearson's HASB scale which form more stable complexes with intermediate metal ions.

The synthesis of PDOX was adapted from Chandler, et al. with minor adjustments. PDOX was characterized by IR, ^{1}H, and ^{13}C-NMR. Characterization showed that pure PDOX was obtained. The first step of the synthesis resulting in 1,10-phenanthroline-2,9-dicarbaldehyde (PDALD) as the product, showed impurities. Therefore, column chromatography was utilized in purifying PDALD. PDALD was then reacted with hydroxyl amine hydrochloride which yielded pure PDOX.

UV-Vis spectrophotometry proved to be a successful tool in determining the protonation constants of PDOX and DIPHEN and the formation constants of the metal-ligand complexes.

Formation constants, logK_1 values, for PDOX compared to 1,10-phenanthroline increased with all metal ions except calcium(II). Exceptional increases were seen in metal ions which had an approximate atomic radius of 1.20Å, such as lead(II). Formation constants of two smaller metal ions were also so high. Copper(II) and zinc(II) had logK_1 values of 10.00 and 8.88, respectively. This is because both copper (II) and zinc(II) are classified by Pearson as being intermediate metal ions which bind preferentially with the nitrogen donor atoms of PDOX.

Fluorescence studies with PDOX coincided with formation constants determined by UV-Vis spectrophotometry of metal-PDOX complexes. Fluorescence increased dramatically upon the complexation of PDOX with lead(II) which has an atomic radius of 1.20Å. For smaller metal ions such as zinc(II) which has an atomic radius of 0.74Å fluorescence does not increase as dramatically. The increase in fluorescence of the metal-ligand complex is due to the CHEF effect in which the lone pair of electrons on PDOX are not able to quench fluorescence when complexing with a metal ion.

DIPHEN, like PDOX, forms five membered chelate rings when complexed with a metal ion as seen in Figure 49, which is the DIPHEN-cadmium complex. This allows for an increase in formation constants when DIPHEN complexes with larger metal ions of approximately 1.00Å. Therefore when compared to 1,10-phenanthroline an increase in logK_1 values was seen for calcium(II), cadmium(II), and lead(II) which are all larger metal ions. A decrease in logK_1 values compared to 1,10-phenanthroline was seen in the two smaller metal ions copper(II) and zinc(II).

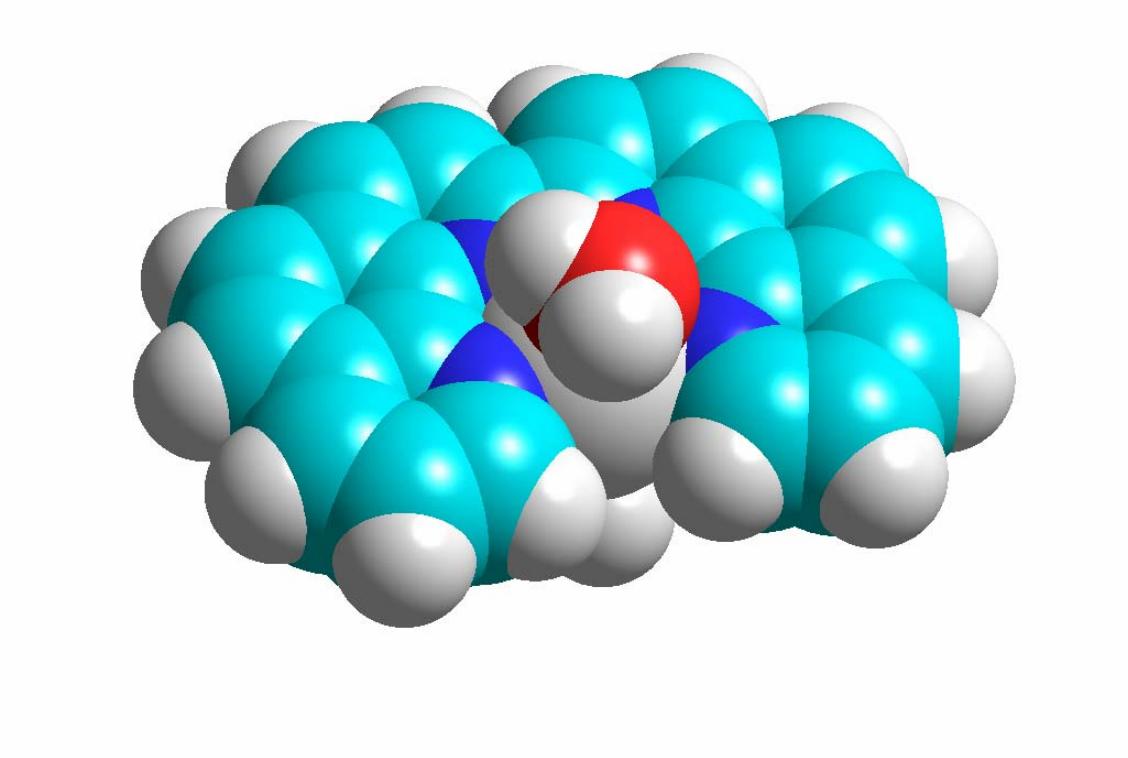

Figure 49: Structure of Cd(II) diphen complex with two axial waters. The structure was generated by MM calculation.

Literature Cited

1. Orvig, C. and M. Abrams, *Chem. Rev*., **1999**. 99. 2201.

2. Lakowicz, J. R. *Principles of Fluorescence Spectroscopy-Second Edition*, Plenum Press, New York, 1999.

3. Godwin H. A., *Cuurent Opinion in Chemical Biology*, **2001**. 5. 223-227.

4. Toth, E., L. Helm, A. E. Merbach, *Comprehensive Coordination Chemistry II*, **2004**. 9. 841.

5. Zhang, S., M. Merritt, D. E. Woessner, R. E. Lenkinski, and A. D. Sherry, *Acc. Chem. Res*., **2003**. 36. 783.

6. Bianchi, A., L. Calabi, F. Corana, S. Fontana, P. Losi, A. Maiocchi, and B. Valtancoli, *Coord, Chem. Rev*., **2000**. 204. 309.

7. Caravan, P., J. J. McMurry, T. J. Lauffer, *Chem. Rev*., **1999**. 99. 2293.

8. Maiocchi, A., *Mini. Rev. Med. Chem*., **2003**. 204. 309.

9. Fulton, D. A., M. O'Halloran, D. Parker, K. Senanayake, M. Botta, and S. Aime, *Chem. Commun*., **2004**. 474.

10. Czarnik, A. W., *Frontiers in Supramolecular Organic Chemistry and Photochemistry*, Weinheim, New York, 1991.

11. Lipscomb, W. N. and N. Strater, *Chem. Rev*., **1996**. 96. 2375.

12. Messerschmidt, A., M. Cygler, and W. Bode, *Handbook of Metalloproteins*, Hoboken, NJ, 2004.

13. Peterson C., Proc. *Natl. Acad. Sci*., **1986**. 83. 7999-8001.

14. Dudev, T., C. Lim, *Chem. Rev*., **2000**. 103. 773.

15. Lippard, S. and J. M. Berg, *Principles of Bioinorganic Chemistry*, University Books, Mill Vally, CA, 1994.

16. Burdette, S. C., *J. Am. Chem. Soc*., **2001**. 123. 7831-7841.

17. Needleman, H., *Annu. Rev. Med*., **2004**. 55. 209-222.

18. Claudio, E. S., H. A. Godwin, and J. S. Magyar, *Progress in Inorganic Chemistry*, **2003**. 51. 1-144.

19. Cram, D. J., "The design of molecular hosts, guests, and their complexes." Nobel Lecture, **1987**.

20. Cram, D. J., *Science*, **1988**. 240. 760-767.

21. Hancock, R. D. and A. E. Martell, *Chem. Rev*., **1989**. 89. 1875.

22. Pearson, R. G. and J. Songstad, *J. Amer. Chem. Soc*., **1967**. 89. 1827-1836.

23. Hancock, R.D., *Accounts Chem. Res*., **1990**. 26. 875.

24. Hancock, R. D. and J. Marsicano, *J. Chem. Soc*., **1976**. 1096.

25. Pearson, R. G., *J. Amer. Chem. Soc*., **1963**. 85. 3533-3539.

26. Chandler, C.J., L. W. Deady, and J. A. Reiss. *J. Heterocyclic Chem.*, **1981**. *18*. 599-601.

27. Angeloff, J. Daran, J. Bernadou and B. Meunier, *Euro. J. Inorg. Chem*., **2000**. 1. 1985-1996.

28. Luckay R., I. Cukrowski, J. Mashishi, J. H. Reibenspies, A. H. Bond, R. D. Rogers, and R. D. Hancock, *J. Chem. Soc., Dalton Trans*., **1997**. 901-908.

29. Martell, A. E. and R. M. Smith, *Critical Stability Constants*, 46. NIST: Gaithersburg, MD, **2003**.

30. Shannon, R. D., *Acta. Crystallogr*., Sect. A, **1976**. A32. 751.

31. Pearson, R. G., *Chemical Hardness*, Wiley, Weinheim, Germany, **1997**.

32. Housecroft, C. E. and Sharpe, A., *Inorganic Chemistry Second Edition*, Prentice Hall, Essex, England, **2005**.

APPENDIX

PDOX 1,10-phenanthroline-2,9-dialdoxime

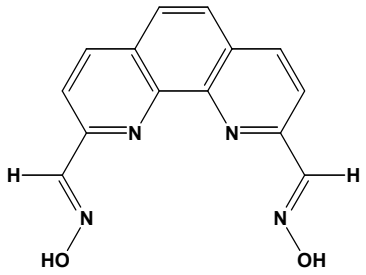

PDALD 1,10-phenanthroline-2,9-dicarboxaldehyde

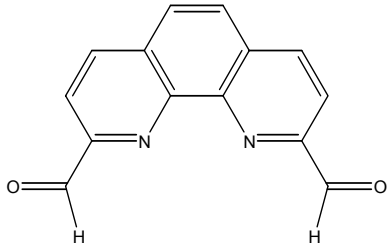

DIPHEN Bis-1,10-phenanthroline

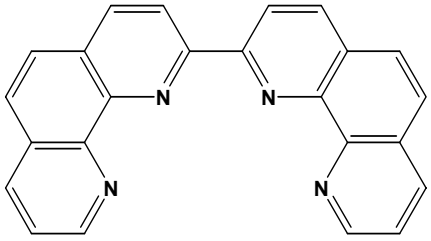

Synthesis of [Pb(PDOX)Cl(ClO4)] crystals

Took 25 mg of PDOX (73 μmol) and dissolved in 400 μL of DMSO (dimethylsulfoxide) and combined in a 10 mL beaker with 43.25 mg of Pb(ClO4)2 dissolved in 100 μL of DMSO. The beaker was placed in a closed chamber with a 50 mL beaker filled with dichloromethane and the crystals were allowed to grow via vapor diffusion. After 3 months the crystal were filter and analyzed.